# SYNTHESIS AND CATION BINDING PROPERTIES OF BIS-BRIDGED CALIX[6]ARENES

THESIS

Presented to the Graduate Council of
Southwest Texas State University
in Partial Fufilment of
the requirements

For the Degree

Master of Science

By

Dustin Blaine Farmer

San Marcos, Texas
December, 1999

# Acknowledgements

I would like to thank most of all Dr. Michael Blanda for all of his help with this research and for much more. His enthusiasm for chemistry as well as in life has taught me a great deal and his confidence in me has made this degree a truly wonderful and growing experience. My best wishes for you, your family, and a future Italian sabbatical.

I would also like to extend my gratitude to my committee members; Dr. James Irvin who's biochemistry and metabolism courses skewed my interest from a biological to a more chemical point of view, and Dr. Walter Rudzinski who has an unique skill of teaching the most complex subject material in an interesting, straight forward, manner.

I would also like to acknowledge Dr. Jennifer Brodbelt and her graduate student Brian Goolsby at The University of Texas for their work on the gas phase competition studies, and Dr. Carl Carrano and Dr. Timothy Higgs for all of the beautiful x-ray crystal structures reported within.

Further appreciation goes out to thank Dr. Norman Dean for his scientific advice and help with the NMR, Stephen Paulson for help with the purification and metal extraction experiments of the bis-pyridinyl calix[6]arene, and Rodney Welsch for computer help and his teachings of the Macintosh operating system.

Final, I would also like to thank my family for their continuous support throughout my entire life.

## Table of Contents

## List of Figures

## List of Tables

# The Synthesis and Cation Binding properties of Bis-Bridged Calix[6]arenes


## Abstract

Calixarenes have been studied and utilized for their molecular recognition properties. A total of four bis-bridged calix[6]arenes have been synthesized and their metal binding properties and structural conformations were studied in solid, solution, and gas phase. Methods of testing include: NMR titrations, liquid-liquid extractions, x-ray crystallography, and electrospray ionization-MS. A dialkylated calix[6]arene was used as the principle starting material which predisposed the four remaining phenolic hydroxyl groups for placement of two bis-electrophiles. The bis-electrophiles were triethylene glycol di-*p*-tosylate , $\alpha,\alpha$-di-bromomethyl-*m*-xylene, and 2,6-bis(bromomethyl) pyridine. All of the compounds tested, with the exception of the bis-xylenyl, formed 1:1 complexes. The bis-xylenyl calix[6]arene is a poor cation binder that is conformationally mobile at room temperature. In contrast the bis-pyridinyl calix[6]arene was a non-selective strong binder of all alkali metal ions. Both bis-bridged aromatic compounds were in a 1,2,3-alternate conformation. Also synthesized were bis-crown-4-calix[6]arene in the cone and 1,2,3-alternate conformation. The calixcrown conformers were selective for the larger alkali metals, cesium and rubidium, with the $Cs^+/Na^+$ selectivity of the cone being 1,400 and that of the 1,2,3- alternate being

144, in solution. Similar results were observed in gas phase competition studies where both conformers exhibited exclusive $Cs^+$ selectivity over $Rb^+$ and a selectivity trend for consecutive larger cations in competition mixtures of $Na^+/K^+$, and $K^+/Rb^+$.

# 1.0 Introduction

## 1.1 Calixarenes

Within the field of organic chemistry, and in the realm of supramolecular host-guest chemistry, there is a family of metacyclophanes called calixarenes. Calix[n]arenes are macrocycles composed of phenolic residues linked at the ortho positions by methylene carbons where [n] represents the number of repeating units in the system.[1]

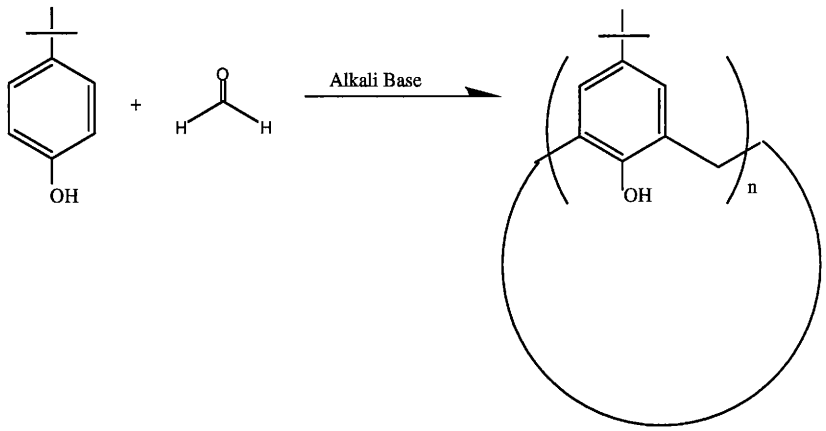


**Figure 1.1** *Synthesis of Calix[n]arene.*[1]

The term calixarene (*calix* = chalice or vase) was coined in 1966 by Dr. David Gustche, who is responsible for major advancements in the calixarene field.[2,3]

Calixarenes with 4, 6, and 8 phenolic residues can be synthesized from t-butyl phenol and formaldehyde by using precise amounts of a specific metal hydroxide base. For example, in the synthesis of calix[4]arene, .045 molar

equivalent of NaOH is used, whereas 0.34 molar equivalent of RbOH or KOH yields predominately calix[6]arene. It has been suggested that the metal of the hydroxide base acts as a template that dictates the calixarene ring number. Calixarenes with 4, 6 and 8 aromatic rings are isolated in the highest yields, are termed the major calixarenes. Until 1993, the minor calixarenes (the cyclic pentamer and heptamer) were obtained as the side products of the major calixarene reactions. This created a development gap, and their advancement has not been as dynamic in comparison to the major calixarenes.[2] Recently, procedural modifications for obtaining the minor calixarenes have been reported which produces yields of up to 20%.[4] Larger calix[n]arenes, with sizes over 20 phenolic residues have been isolated by Gutsche and coworkers. Informally, these compounds are termed 'Texarenes', since the bulk of the research was carried out in Gutsche's laboratories located in the state of Texas.[3] Most extensively researched are the calix[4]arenes, mainly due to their structural simplicity, and tunable guest accommodating features achieved through selective functionalization. Applications of calix[4]arene in catalysis[5], ion separations[6], and sensors[7] are centered around their molecular recognition properties. More recently, shifting interests in novel calix[6]arene research has generated a need for selective synthetic functionalization strategies and conformational manipulation.

## 1.2 Calix[6]arene

### 1.2.1 Representation of Orientation

The numbering of carbons in the calix[6]arene framework is shown in Figure 1.2.

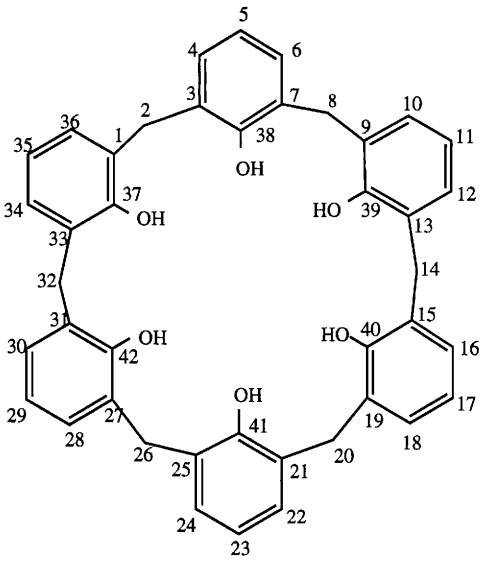


**Figure 1.2** *Carbon Numbering of Calix[6]arene-36,37,38,39,40,41,42 hexol*

Calix[n]arenes are conformationally mobile compounds, where each phenolic residue can undergo complete ring inversion, by rotation through the macrocylic annulus. Conformational mobility makes it possible to fashion various unique supramolecular environments. There are several ways to depict the orientation of calix[6]arenes. The most common conformational description is a series of six abbreviations, where a reference aryl ring is assigned in an up position, followed by each consecutive ring's relative orientation around the skeleton, where u = up, d = down, o = out, di = down in, up = up out and so on.

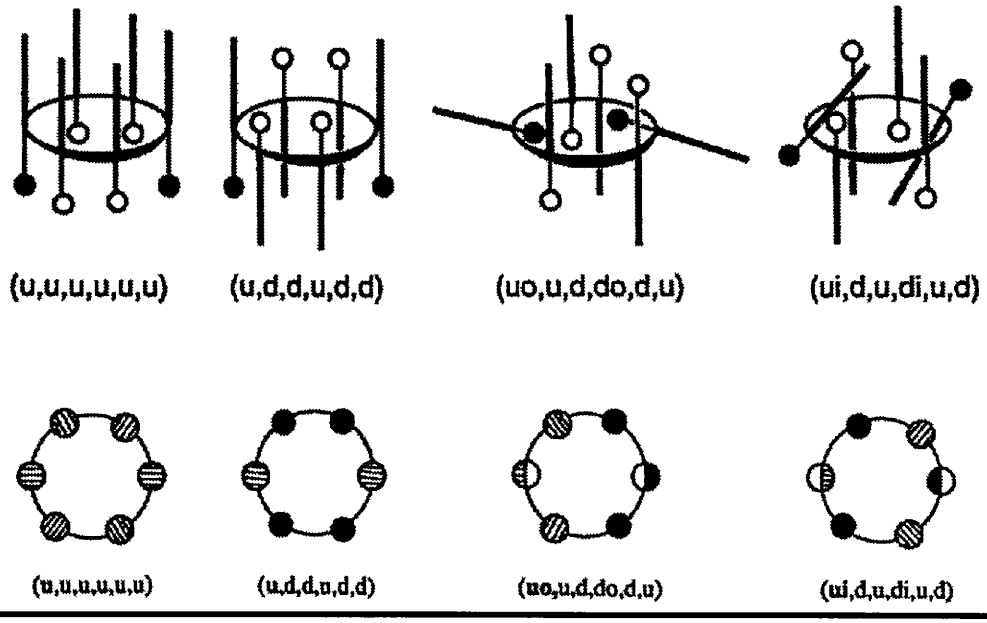


**Figure 1.3** *Representations of cone, 1,4-Alternate, 1,2,3-Alternate, and 1,3,5-Alternate conformations respectively.*

The designation for a cone conformation would be (u,u,u,u,u,u); however, a more precise designation would be used to describe a pinched cone (uo,u,uo,uo,u,uo), having a concave bowl shape. Another common conformation is the 1,2,3 alternate (uo,u,d,do,d,u,), where three neighboring rings are in an up position and the other three are inverted. In addition, each phenolic ring is given an alphabetical designation (A,B,C,D,E,F) to simply state which ring(s) are being discussed relative to a reference ring. In the 1,2,3 alternate conformation the reference ring is the first ring in the three ring alternate sequence (u,uo,u,d,do,d) where the A ,B and C rings are up and the D, E and F rings are down.[3] In solution, calix[6]arenes exist primarily in cone and 1,2,3-alternate conformations regulated by the hydrogen bonding at the lower rim. The cone conformation

allows the maximum intramolecular hydrogen bonding. When the H-bonding is reduced, the cone conformation converts to the 1,2,3-alternate conformation. This is achieved by changing the experimental conditions including temperature and solvent polarity or alkylation of the hydroxyl groups.[8]

The relative orientation of the rings arises from rotation around the $ArCH_2Ar$ bonds between each ring. When the two neighboring rings next to each other are in (u,u) orientation the $ArCH_2Ar$ carbon has syn orientation, and when the rings are opposite (u,d) to each other they are called anti(Figure 1.4). A significant aspect of these types of carbons is that they can exhibit unique chemical shift in $^{13}C$-NMR spectra which can be employed as a diagnostic tool to determine conformation. According to a general rule proposed by Gutsche[1], in $^{13}C$-NMR, calix[6]arenes with all syn or all anti methylene carbons have a $\Delta\delta < 1$ whereas mix of anti and syn methylene carbons typically have a $\Delta\delta > 3$ ppm.[3]

### 1.2.2 Dihedral angles

The most critical feature in determining the conformation of a calixarene is the value of the dihedral angles, $\phi$ and $\chi$, as defined by the sequences C1-C2-C3-C4, and C2-C3-C4-C5 respectively (Figure 1.4)[9]. This type of analysis requires x-ray crystallographic data. If the two adjacent aryl rings are in A orientation, $\phi$ and $\chi$ have opposite signs whereas in orientation B the signs are the same.

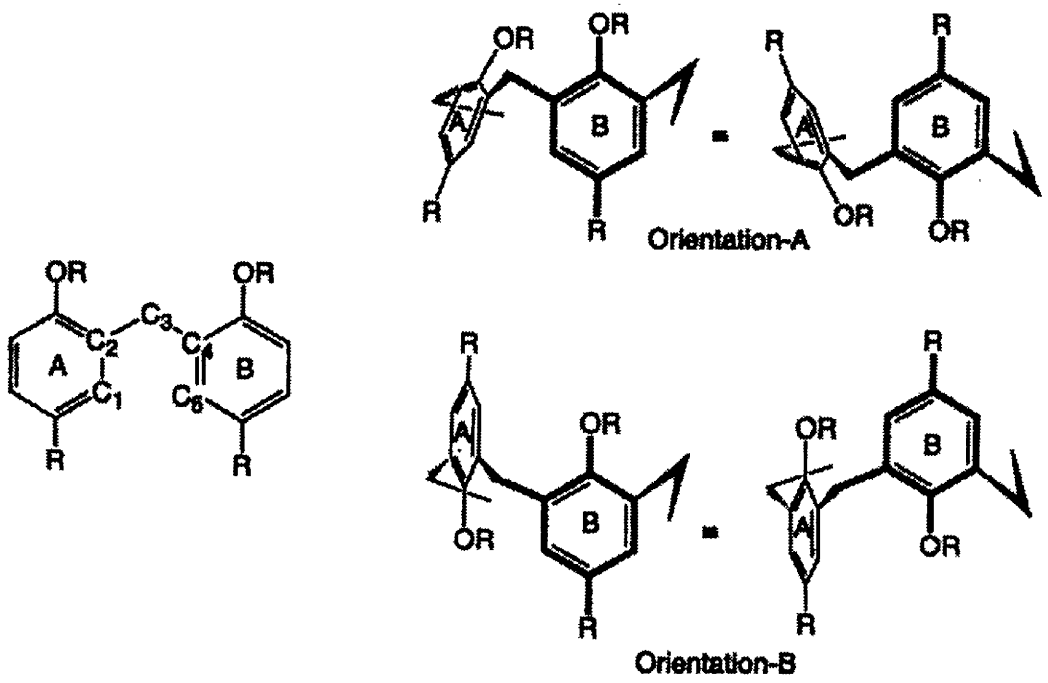


**Figure 1.4** *Carbon designations for dihedral angle calculations, and syn(A) and anti(B) oreintations of the $ArCH_2Ar$ carbons.*

## 1.3 Immobilized Bridged Calix[6]arenes

### 1.3.1 Ring Interconversion

In the cone conformation there is an upper rim (t-butyl positions), and a lower rim (hydroxy), where most functionalization takes place. Conformational ring interconversion occurs by the upper or lower rim of a phenolic residue rotating through the annulus of the calixarene as seen in Figure 1.5.

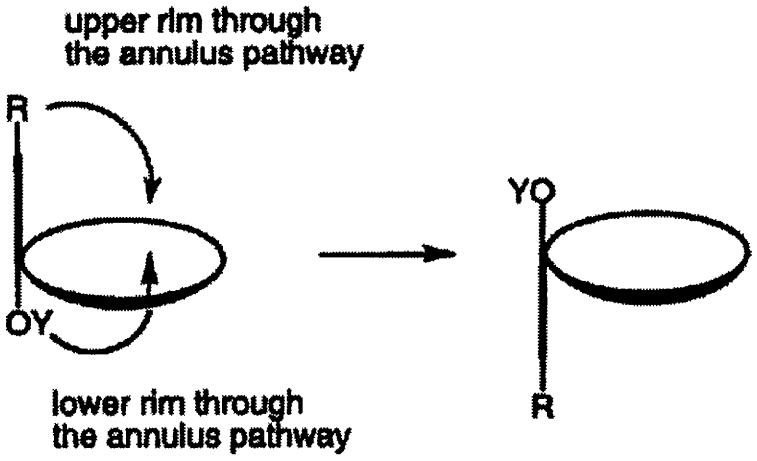


**Figure 1.5** *Pathways for ring interconversion*

Upper rim ring inversion of *p-tert*-butylcalix[6]arene can occur when the upper rim *t*-butyl groups are still intact, prior to dealkylation. In calix[6]arene, the lower rim, through-the-annulus ring interconversion pathway is relatively low in energy, while the energy barrier for the upper rim pathway is 21 kcal/mol at 55 °C.[10] In lower rim substitution, sufficiently larger groups are required to hinder lower rim ring interconversion. Threshold studies involving hexabenzyloxycalix[6]arene have shown that lower rim ring interconversion is allowed while the hexa *p*-cyanobenzyloxycalixarene does not interconvert.[11]

### 1.3.2 Bridging Effects on Ring Interconversion

There are several avenues to conformationally immobilize or freeze the calix[6]arene. The most common method to limit flexibility and hinder ring interconversion is functionalization of the lower and upper rim with bulky

substituents. The appended groups must be bulky enough to sterically hinder both pathways of ring interconversion. An alternative way to achieve immobilization is intramolecular bridging, or strapping of the calixarene. Most bridging is done on the lower rim, which hinders both upper and lower rim rotations by securing or tethering the rings of the calix[6]arene's framework. Bridging can provide varying degrees of conformational rigidity depending on the flexibility and length of the bridging unit. Lesser rigidity is observed in Figure 1.6 where an example of a triply bridged calix[6]arene exhibits complete conformational inversion above - 23 ˚C from a cone to a partial cone conformation.[12]

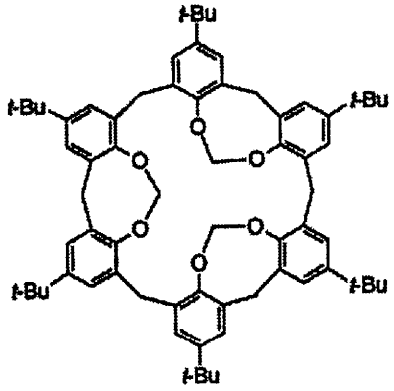


**Figure 1.6** *Conformationally mobile triply bridged calix[6]arene.*

Figure 1.7 shows cases where a single bridge on the lower rim still permits conversion from a cone to a 1,2,3-alternate conformation by threading the strap through the annulus.[13]

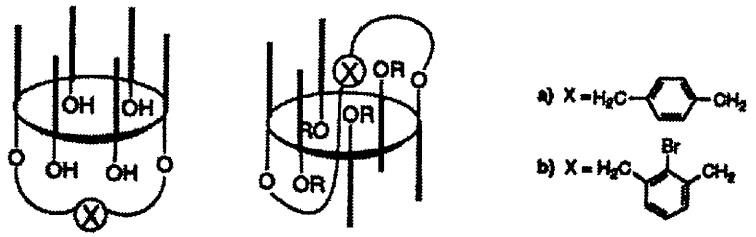


**Figure 1.7** *Single bridged calixarene converting from a cone to a 1,2,3,-. alternate conformation*

An example of extreme rigidity is observed in a calix[6]arene which has a triple linked cap placed on the lower rim (Figure 1.8). These are called cryptocalix[6]arenes and have been studied by Shinkai and coworkers.[14]

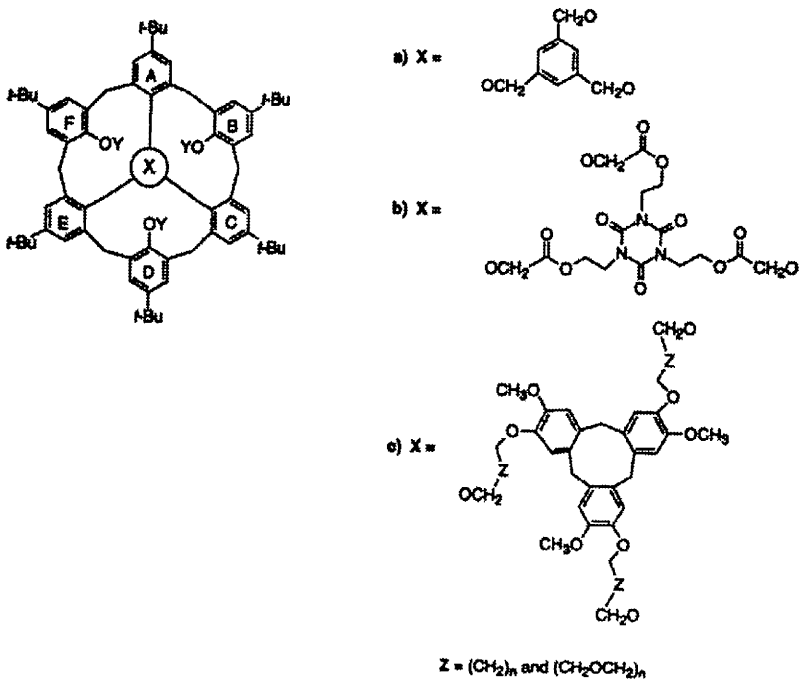


**Figure 1.8** *Cryptocalix[6]arenes and three trifunctionalized capping units*

Most of the bridged calix[6]arenes have been subjected to temperature dependent NMR studies to get a sense of the energy requirements to induce flexibility from a more rigid state.

### 1.3.3 Bridged Calixcrowns

Crown ethers are cyclic polyethyleneoxy structures capable of binding a variety of cations with different sizes and topographics. Originally pioneered by Dr. Donald J. Cram in the 1970's, the selectivity of crown ethers can be regulated by the size of the polyethyleneoxy ring. For example, the crown-4 cyclic structures selectively coordinate $Na^+$ and $Li^+$, while the crown-5 and crown-6 coordinate $K^+$ and $Cs^+$ respectively. Calixcrowns are macromolecular hybrid structures composed of calix[n]arenes and crown ethers which have been demonstrated to be very effective complexing agents for alkali and other metal ions.[14] Incorporation of crown ethers onto calixarenes was introduced initially by Ungaro and coworkers in 1983. Calixcrowns have been constructed from all four conformational isomers of calix[4]arenes (cone, partial cone, 1,2- and 1,3-alternate) as well as calix[5]- and calix[6]arenes.[14,15] Since they contain a single crown ether strap, the mono-bridged calixcrowns all form 1:1 complexes. In addition to the calixcrowns which have only a single crown moiety, there are numerous examples of calix-bis-crowns which have been primarily composed of calix[4]arenes and two oxa-or azacrown units.[16] These ditopic, bis-bridged calixcrowns generally form 2:1 (guest to host) adducts when they are completely complexed. The introduction of a second bridging unit also increases the rigidity of the calix[4]arene framework.

X-ray crystal structures for the complexes of $K^+$ with the cone (a) and partial(b) cone conformers reveal that the K-O bond distances are shorter in the

cone complex compared to the partial cone leading to an assumption that the cone-$K^+$ conformer has a tighter fit (Figure 1.9).

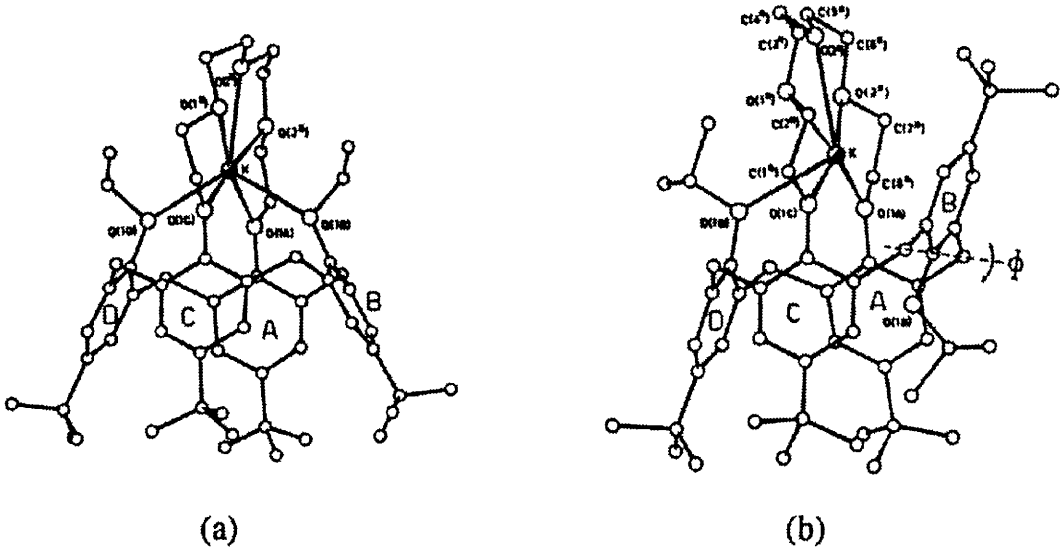


(a) (b)

**Figure 1.9** *Cone(a), and Partial cone(b) calixcrown complexes with $K^+$.*

However, it was shown that the partial cone actually forms a tighter complex due to the cation-$\pi$ interaction between $K^+$ and the phenyl ring (B)[17]. A similar $\pi$ interaction was seen in some of the x-ray crystal structures acquired in our research. Because of the merger of two modifiable host molecules, calixcrowns offer synergistic versatility in selectivity and affinity properties associated with both types of compounds.

## 1.4 Thesis Proposal

Calix[6]arenes have not been studied as much as the calix[4]arenes primarily because they are more complex, due to the increase in ring size and

flexability. Even though calix[6]arenes have yet to realize their full potential, strategies for the development of new processes applicable to calix[6]arenes are destined to be explored and are warranted.

The purpose of this research was to synthesize rigid calix[6]arenes and study their metal binding properties. An A, D-dialkylated calix[6]arene[18] was used in order to predispose the four remaining phenolic hydroxyl groups for placement of two bridging units to create rigid calix[6]arenes. Two different conformational isomers were produced by placement of aromatic[19] and crown ether[20] containing straps connecting pairs of rings separated by the alkylated rings.

Conformational arrangement of each host were established and investigations of the relationships between their supramolecular isomeric structural differences and their metal binding properties were made using NMR titrations, UV metal salt extractions, and x-ray crystallography. In addition, a discrepancy in a general rule used for determining conformation of calixarenes was observed.

**1.5 Alkali metal binding studies**

We have synthesized a small family of bis-bridged calix[6]arenes, three of which take on a 1,2,3-alternate conformation and one which adopts a cone conformation. Analysis of the complexes were performed in solid, solution, and gas phases. NMR experiments were also used to determine activation of free energy relating to conformational flexibility and metal decomplexation of ions. X-

ray crystallography data was obtained on all four compounds, however two of the four structures were not fully solved. Liquid/ liquid extractions were done by existing methods using aqueous picrate metal salts $Li^+$, $Na^+$, $K^+$, $Rb^+$, and $Cs^+$ alond with the host dissolved in organic solutions.[21] Similar extraction studies have been performed on other calixarenes as well as on crown ethers and other non-polar host molecules.[22]

## 2.0 Synthetic Strategy

### [2.1] 5, 11, 17, 23, 29, 35-hexa-*p-tert*-butyl-37,38,39,40,41,42-hexahydroxycalix[6]arene Synthesis (1)

The preparations and properties of compound **1** and **2** have been well known for several years.[1] The principle starting material *p-tert*-butylcalix[6]arene was obtained in high yields from the RbOH base condensation reaction of *p-tert*-butylphenol and paraformaldehyde in refluxing xylene (see Figure 2.1).[2]

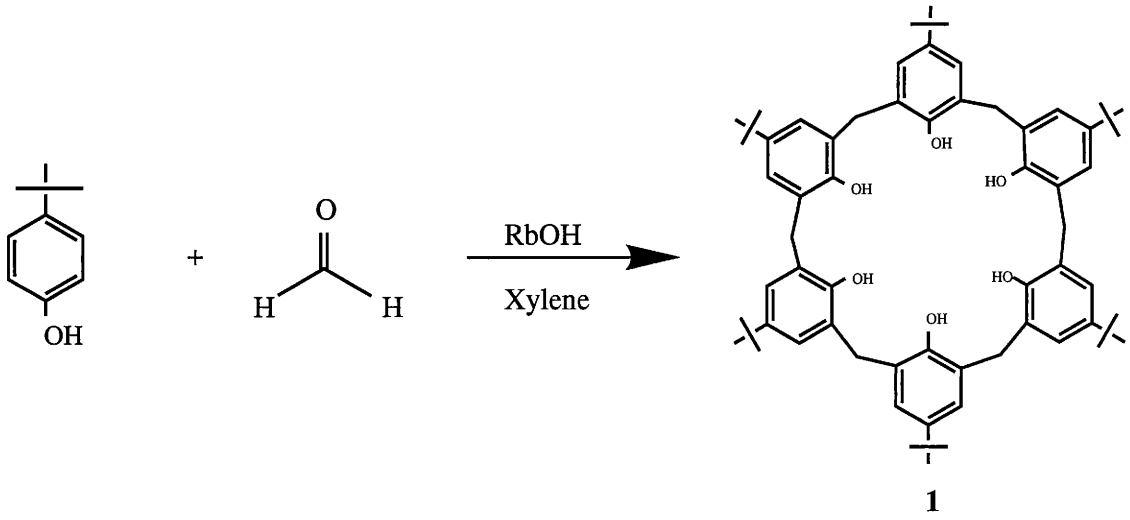


**1**

**Figure 2.1** *Synthesis of compound 1*[1]

Precise amounts of RbOH (0.45 molar equivelents) are used for preparation of calix[6]arene. The alkali metal hydroxide base is believed to have a template effect in dictating the calixarene ring number. Generally larger alkali metal hydroxides produce larger calixarenes, where NaOH produces calix[4]arene and CsOH produces the calix[8]arene. The crude reaction mixture washes for calix[6]arene tend to be more difficult than that of the calix[4]arene due to

excessive emulsions that occur during aqueous washes and a decreased solubility in halogenated solvents.

### [2.2] 37,38,39,40,41,42-hexahydroxycalix[6]arene synthesis(2)

The synthesis of **2** is a reverse Frediel-Crafts alkylation using $AlCl_3$ as the catalyst, in toluene (see Figure 2.2). This standard procedure removes the t-butyl groups from most of the different sized calixarenes.[2, 3] The removal of the t-butyl groups characteristically allows for more flexibility and upper rim ring interconversion.

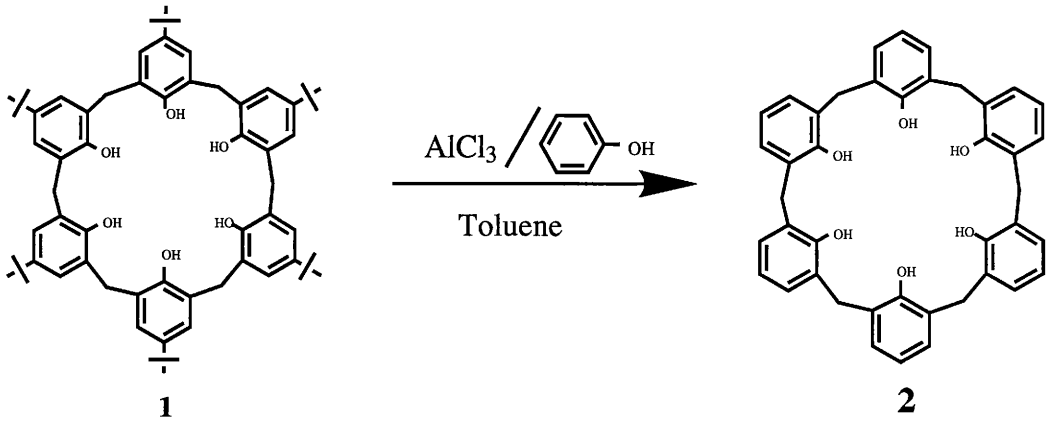


1 2

**Figure 2.2** *Synthesis of compound 2* [2, 3]

Dealkylation of the upper rim, prior to further functionalization, provides the basic starting compound from which all six positions of both the upper and lower rims are accessible for chemical modification.

**[2.3] 37,40-Diallyloxy-38,39,41,42-tetrahydroxycalix[6]arene synthisis (3)**

Bis-bridged calix[6]arenes with triethylene glycol, *m*-xylenyl, and 2,6-pyridinyl, (**4,5,6,** and **7**) were prepared from 37,40-diallyloxycalix[6]arene, **3**. The starting material was obtained in excellent yield (96%), by selective alkylation on the phenolic oxygens of the A and D rings of compound **2** using allyl bromide in the presence of $K^+(CH_3)_3SiO^-$ (Figure 2.3).[18]

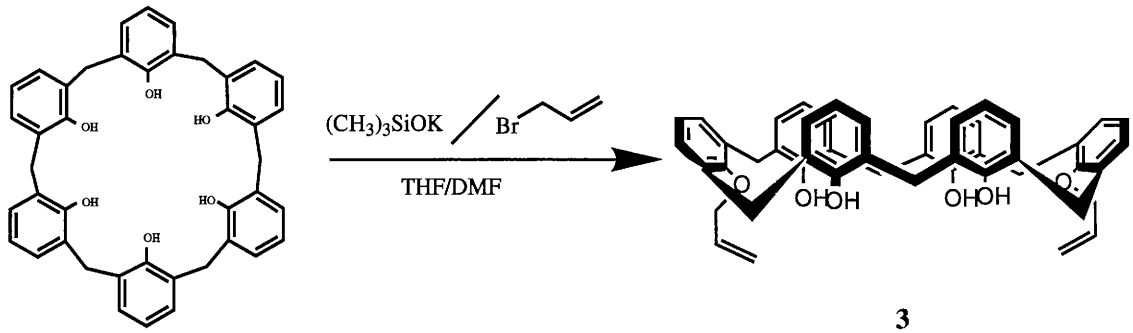


**Figure 2.3** *Synthesis of compound **3***[18]

Placement of the allyl groups on the lower rim of the A and D rings predisposed the remaining B, C, E and F rings for bridging with bis electrophiles. The $^1$NMR spectrum of **3** contains a sharp singlet for the $ArCH_2Ar$ hydrogens indicting a conformationally mobile skeleton which allows for several different possibilities of the ring orientation prior to bridging attachment.

## 2.4 Bis-Bridged Calix[6]arenes

### 2.4.1 General Conditions

Reaction conditions for all of the bridging reactions required the same solvent, base and bridging reagent stoichiometry. Approximately 1 g of compound **3** per 100 mL of a THF/DMF (10:1) solvent mixture was used. High dilution favors intramolecular bridging over intermolecular bridging which would result in the linking of two molecules of calix[6]arene. Sodium hydride (NaH), 60% in a mineral oil dispersion, was used as the base. All of the difunctionalized bridging reagents used were in a 2.4 molar excess relative to compound **3**.

After bridging takes place, the conformation of the calixarene framework is locked where the rings can no longer rotate through the annulus. Two families of isomers can potentially be produced, those with the bridging groups one side of the calix[6]arene (u, u, u, u) and those on opposite sides of the calix[6]arene (u, u, d, d). Within each family, the alkylated A and D rings can be orientated up or down. Considering all of these structural variations, there are six conformational isomers possible for the B-F, C-E bis-bridged family (Figure 2.4).

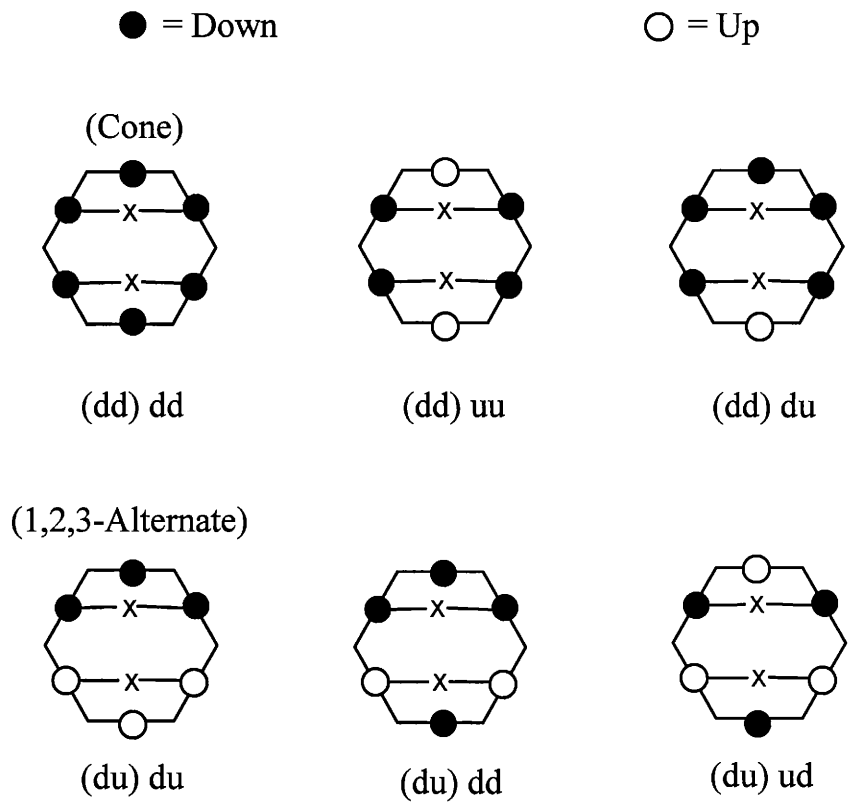


**Figure 2.4** *Possible B/F-C/E Bis-Bridged Isomers.*

### [2.4.2] 37,40-Diallyloxy-(38-42),(39-40)-biscrown-4-calix[6]arene (4) and (5)

When **3** was treated with tri(ethylene glycol)-di-*p*-tosylate and NaH in THF/DMF, approximately equal amounts of **4** and **5** were isolated.

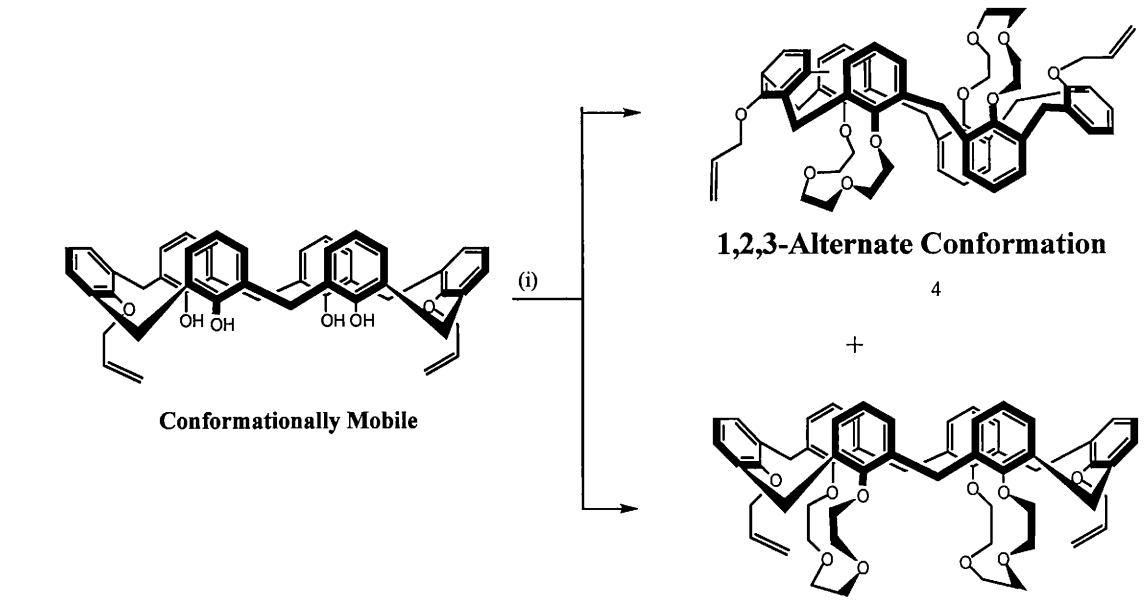


**Figure 2.5** *Synthesis of compound **4** and **5***

The total amount of the bis-crown-4-calix[6]arenes was consistently 20-30% of the reaction mixture and they were separated and purified using column chromatography. Thin layer chromatography (TLC) of the crude reaction mixture does not reproduce the same $R_f$ value as does the purified compound **4**. During the initial purification of **4**, a spot with the $R_f$ value of .73 appeared in a fraction unseen in the crude TLC sample ($R_f$ = 1, solvent front). An explanation of this phenomena could be that it sequestered an adduct in the crude reaction mixture that was removed during the bulk purification. In addition, the cone conformer (**5**), appeared as a smear that would not form one constant spot even when purified crystals were redissolved and subjected to TLC analysis. When the reaction

conditions were changed to $Cs_2CO_3$ as the base in acetonitrile, the reaction mixture became more complex and purification of **4** and **5** proved too difficult. Tetra and penta(ethylene glycol)-di-p-tosylate were also used in attempts to create additional bis-bridged compounds, however the desired compounds were never isolated. One explanation of why longer crown ether straps would not yield intramolecular bridging is that there is unfavorable entropic effect of finding the free phenolate oxygen during the second electrophilic attack completing the intramolecular bridge.

### [2.4.3] 37'40-Diallyloxy-(38,41)-(39,42)-bis-m-xylenyloxycalix[6]arene (6) and 37'40-Diallyloxy-(38,41)-(39,42)-bis-(2,6-dimethylpyridinyloxy)calix[6]arene (7)

Compound **3** was treated with 6 molar equivalents of NaH in a 10:1 THF/DMF mixture and the appropriate strapping reagent ($\alpha,\alpha$-dibromo-*m*-xylene) or (2,6-dibromomethylpyridine) in a 2.4 molar excess relative to the dialkylated calixarene **3** (see Figure 2.6). The reaction of **6** was refluxed for 24 h while **7** was allow to stir at room temperature for 5 days at room temperature primarily to avoid decomposition of the (2,6-dibromomethylpyridine) reagent (m.p. >85-87° dec.).

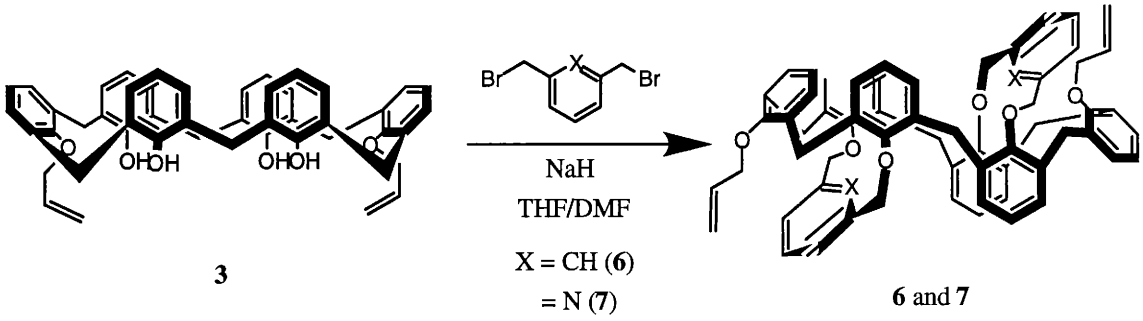


**Figure 2.6** *Synthesis of compounds **6** and **7**.*

The bridging reactions were surprisingly efficient, as **6** and **7** were isolated in 60-65% yields by column chromatography. Only the 1,2,3-alternate conformers of the bis-strapped calix[6]arenes were isolated. While **6** was isolated on polar silca gel as the solid suport, the purification of **7** required less polar, aluminum oxide.

# 3.0 Results and Discussion of Compounds 4 and 5

## 3.1Conformational Analysis of 1,2,3-Alternate Isomer (4).

### 3.1.1 X-Ray Crystal Structure (4)

The 1,2,3-alternate conformation of **4** was confirmed using x-ray crystallography.[24] Figure 3.1 shows that the two crown moieties are on opposite sides of the molecule and that the B-F and C-E rings are bridged.

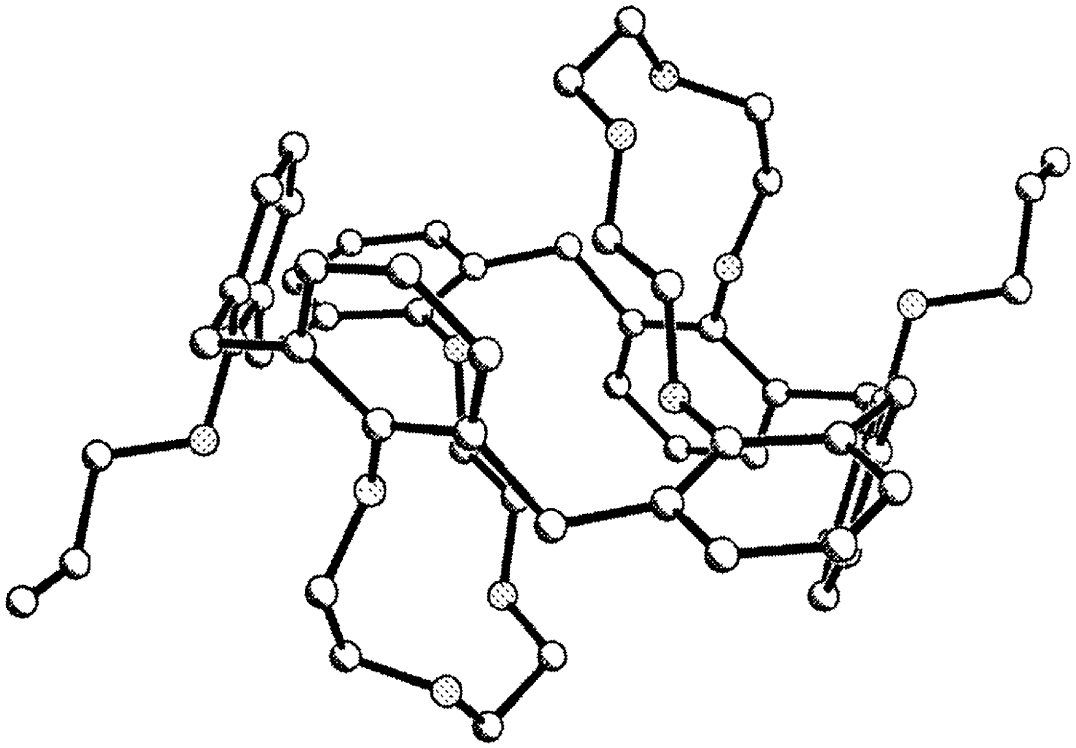

**Figure 3.1** *Partially solved crystal structure for compound **4**.*

A 30-membered ring containing eight oxygen atoms is created by the two polyether straps and atoms of the four bridged calixarene rings. The four oxygen atoms of the bridged calixarene rings are nearly coplanar with the remaining

ether oxygen atoms situated in the polyether straps above and below the plane. The conformation can be further described using the following stereochemical notation (u, uo, do, d, do, uo) relative to the A ring.

### 3.1.2 NMR Analysis (4)

The 1,2,3-alternate conformation of **4** in solution could readily be determined from one- and two-dimensional NMR spectroscopy ($^{1}H$, $^{13}C$, $^{1}H/^{1}H$ COSY, $^{1}H/^{13}C$ HETCOR in appendix spectra 1-4). In the $^{1}H$-NMR spectrum (Figure 3.2), the diagnostic conformational indicator was the signal pattern observed for the two types of $ArCH_2Ar$ protons.

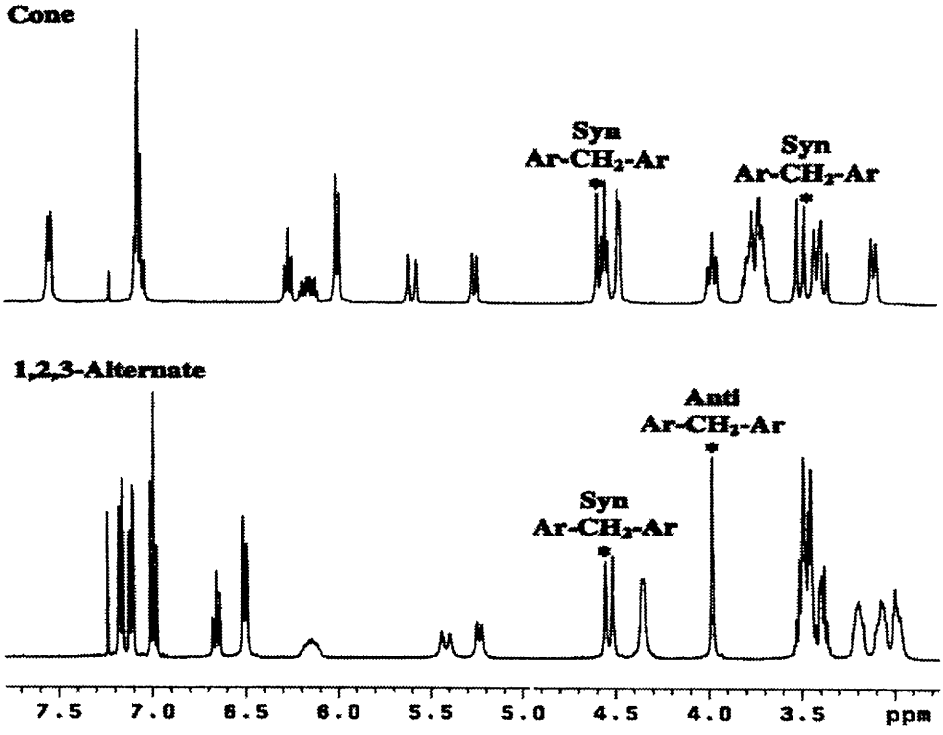


**Figure 3.2** *$^{1}H$-NMR spectra of compound **4** and **5** showing shifts of the methylene carbons in syn and anti orientation.*

The methylene protons between syn-oriented aromatic rings appeared as an AB quartet and had a $\Delta\delta$ = 1.05 ppm, similar to that observed for the endo- and exo- protons of cone calix[4]arenes.[2,3] The $ArCH_2Ar$ hydrogens between anti-oriented rings appeared as a singlet with half the intensity of the AB quartet. Corroborating evidence for the two types of $ArCH_2Ar$ methylene carbons was obtained from the $^{13}C$ spectrum in which there were two signals observed at 31.55 and 30.13 ppm (intensity 1:2, $\Delta\delta$ = 0.42 ppm at RT). It is interesting that the 1,2,3-alternate conformation of **4** is in violation of the $^{13}C$ rule for determining conformations of calix[6]arenes.[11] Normally, a $\Delta\delta$ smaller than 1ppm means that the $ArCH_2Ar$ carbons are either all syn or anti.

The presence of just 10 signals for all of the aromatic carbons in the $^{13}C$ NMR spectrum of **4** entails of its symmetry; $C_2$ and i. The same symmetry elements also operate on the crown ether moieties, thus only three signals were observed for the 12 methylene carbons of the crown-4 units. The COSY and HETCOR spectra indicated that the methylene hydrogens of the crown units are diastereotopic with the $\Delta\delta$ between pairs of signals ranging from 0.086-.260 ppm.

## 3.2 Conformational Analysis of Cone Isomer (5).

### 3.2.1 X-Ray Crystal Structure of Cone(5)-Cesium Complex.

The x-ray crystal structure of cone-cesium complex (Figure 3.3) verified that the calix[6]arene framework was indeed in the cone conformation (ui, uo, uo,

ui, uo, uo) and that the two crown units cooperatively bound the cesium ion. Further inspection of the cone conformer 5, using Corey-Pauling-Koltun (CPK) models, indicated a rigid preorganized free host calix[6]arene. The only significant flexibility avalible to the conformer was in the two alkylated rings. The two alkylated rings appear flexibile enough to move from the up in (ui) position to the up out (uo) position.

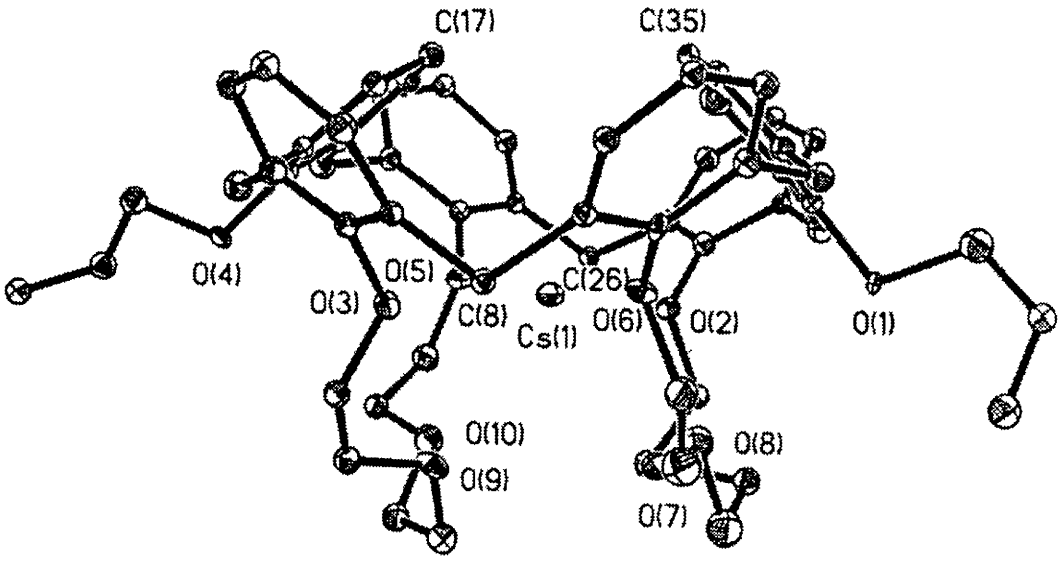


**Figure 3.3** *Crystal structure of compound **5** - $Cs^+$ complex.*

The para carbons (C5, C11, C23 and C29) of the B, C, E and F rings define a rectangular plane with average dimensions of 11.45 Å x 5.54 Å. In the solid state the A and D rings come within 3.885 Å of each other (C17-C35). The coordination sphere around the metal looks asymmetric in that there are apparently no ligands above the metal. However the A and D rings of the

calixarene are canted over the top of the cavity and their centroids come within 3.78 Å of the cesium cation. This is slightly farther than the π-metal distances reported in some calix[4]crowns derived from the 1,3-alternate conformation,[25] but not unreasonable to conclude that long range interactions between the cation and the A and D rings are present in the solid state. In fact, one explanation for their proximity is that they are held in position by interactions with the cesium ion.

With the addition of the two polyether chains at the lower rim, the whole structure has a deep bowl shape with the eight oxygens of the two parallel crown-4 units directed towards the center. The four phenolic oxygens of the bridged rings (O2, O3, O5 and O6) are almost coplanar as evidenced by the -12° dihedral angle between the planes defined by O3-O2-O6 and O5-O6-O2. The lengths of the plane are defined by the O2-O6 and O3-O5 distances (7.14 Å and 7.73 Å, respectively) and the widths are defined by the O2-O3 and O5-O6 distances (3.52 Å and 3.36 Å, respectively). The four remaining oxygens in the ether chains are below the plane while the oxygen atoms of the A and D rings are directed away from the cavity.

The Cs-O bond lengths to the phenolic oxygens vary from 3.407 Å to 3.611 Å with the average being 3.523 Å. The four bond angles between the cesium ion and the bridged phenolic oxygens are 119.34° (O3-Cs-O5), 124.41° (O2-Cs-O6), 57.23° (O2-Cs-O3) and 59.75° (O5-Cs-O6) and add up to just slightly more than 360°(angle summation = 360.73°). The cesium cation is coordinated to all eight oxygen atoms and lies essentially in the center of the

phenolic oxygen plane. As seen in figure 3.3 and 3.4, the cesium ion is coordinated on its bottom side to the four ether oxygens atoms (O7, O8, O9 and O10) in the two crown straps. The average crown Cs-O distance is 3.189Å which is shorter than that of the phenolic oxygens, with the individual distances ranging from 3.093-3.299 Å.

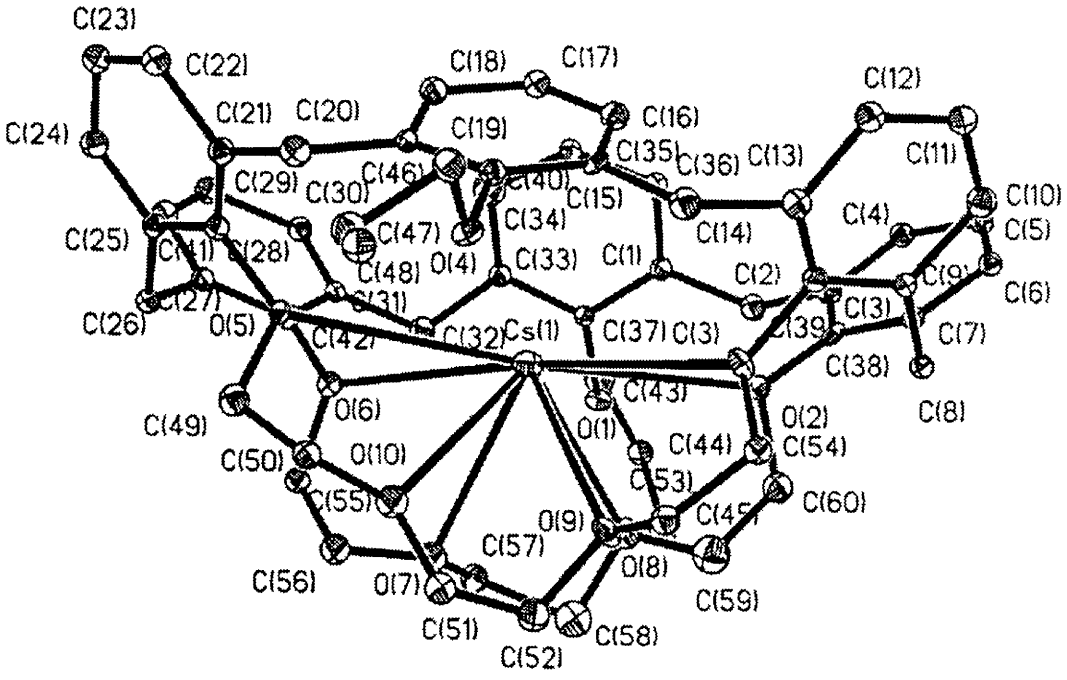


**Figure 3.4** *Crystal structure of compound **5** (side view).*

The cesium ion could possibly enter the cavity through the calix opening or through an opening between the crown units. The molecular model of **5** suggests that the through-the-calix pathway for complexation is favored. Once the cesium

is bound by the oxygen atoms, the A and D rings are then held in over the cavity by the π-metal interactions.

### 3.2.2 NMR Analysis of 5

The cone conformation of isomer **5** was most clearly demonstrated by presence of two AB quartets for the $ArCH_2Ar$ protons (2:1 ratio) in the $^1H$ NMR spectrum (Figure 3.2A). The $\Delta\delta$ between the AB pairs was 1.08 and 1.18 ppm, respectively and the coupling constants (J = 16.4 Hz) were similar to those observed for calix[4]arenes locked into the cone conformation.[2,3] Even though all of the $ArCH_2Ar$ carbons are situated between syn-oriented aromatic rings, there are two different types: those flanked only by the bridged rings and those flanked by the allyl-functionalized rings (30.88 and 27.09 ppm, respectively). The $\Delta\delta$ of 3.79 ppm is again contrary to the general rule that when the $\Delta\delta$ is greater than 3 ppm both syn and anti orientations are present in the calix[6]arene.[11] In this case it is the syn oriented methylene carbons between the bridged ring pairs that are shifted to higher than normal fields by approximately 3 ppm. Similar to the 1,2,3-alternate conformer, the molecule has a high degree of symmetry as evidenced by the relative simplicity of the $^{13}C$ spectrum in which only 10 aromatic signals and three for the crown units were observed. A comparison of the chemical shifts of the para and meta hydrogens of the A and D rings in **4** (6.66 and 6.51 ppm) and **5**(6.29 and 6.03 ppm) suggest that the rings are canted inward and these protons are shielded by the B, C, E and F rings. Just as in isomer **4**, the

methylene hydrogens of the crown moieties are diastereotopic, but the $\Delta\delta$ values between diastereotopic hydrogens are larger (0.89 ppm).

## 3.3 NMR Studies of Host/Guest complexation

### 3.3.1 NMR Fast and Slow Exchange

Most of the NMR signals of each host, shifted as a result of binding metal ions. On the NMR time scale, the rate of complexation/decomplexation can occur in fast or slow exchange. In fast exchange the signals are a weighted average of both free and complexed host that shift to higher or lower fields. The final location of the signal limits out at excess guest concentrations. Slow exchange is sometimes indicative of a stronger binder, and the resulting spectra show separate signals for both the complexed and free host.[26] $^1$H-NMR spectroscopy was used to investigate the stereochemical changes of the hosts, and stoichiometries of the complexes formed between **4** and **5** host and alkali metal ions. The crown isomer **4** was in rapid exchange with $Li^+$, $Na^+$, $K^+$ and $Rb^+$ ions (appendix 16) while **5** was in rapid exchange with its $Li^+$, $Na^+$ and $K^+$ complexes (appendix 17). The exchange rate for complexation was slow on the NMR time scale when host **4** bound cesium and when host **5** bound cesium and rubidium. Both hosts **4** and **5** appear to show a preference for binding the larger cesium and rubidium ions over the smaller alkali metals

### 3.3.2 Complexation Stoichiometry via NMR

With two crown ether straps on opposite sides of the molecule, it was speculated that **4** might form 2:1 (guest to host) complexes. This question was answered using the method of continuous variations (Job plot) to probe the binding of the relatively small sodium cation.[26] The Job plot method for determining the guest to host ratio was performed by fixing the total concentration constant, while changing the host to guest ratio. By plotting the change in chemical shift of the carbons in the crown moiety multiplied by the mole fraction of the host versus the mole fraction of the host, the resulting curve maximizes at the mole fraction when the stoicheometric host/guest complex is most abundant. For compound **4** the resulting curve (Figure 3.4) maximizes at 0.5 indicative of a 1:1 complex. The sodium cation was chosen for this study based on a calixcrown-4 compound reported by Shinkai that exhibited high sodium selectivity.[27] Under fast exchange conditions, the changes in the chemical shifts of the crown methylene carbons in the $^{13}C$ NMR spectrum of **4** were used to monitor the complexation process.

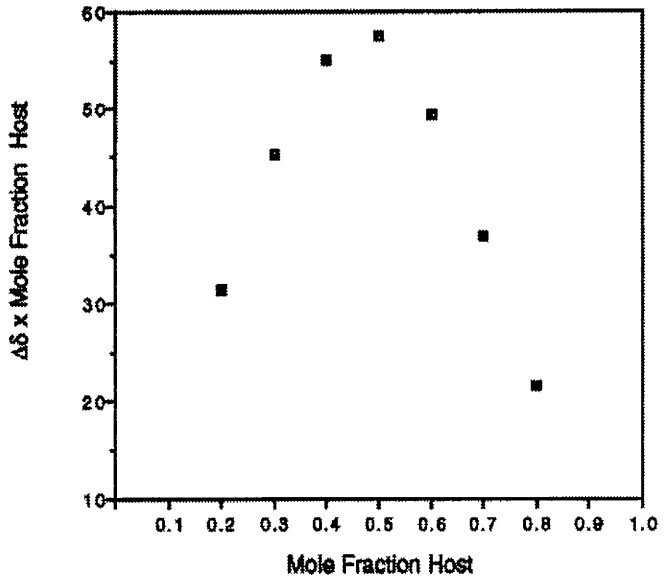


**Figure 3.5** *Job plot of $Na^+$ binding for compound **4**.*

Even though the crown-4 units are on opposite sides of the molecule, they may coordinate metal ions cooperatively, unlike most calix-bis-crowns, which form 2:1 complexes.[16] However, this does not rule out the possibility of a sodium cation in fast exchange between the crown loops on opposite sides of the molecule. Room for two smaller cations exist within the larger macrocylic structure but, the electrostatic repulsion would be unfavorable. Inspection of CPK molecular models suggested that the sodium ion is best coordinated by the four planar phenolic oxygen atoms. The four strap oxygen atoms appear to be too remote for bonding interactions with small cations. The cooperative nature of the two crown-4 units reverses the binding selectivity of the crown-4 units If they operate

independently, there is then a high sodium selectivity, but when they act in concert, the hosts have high selectivity for larger cations.

### 3.4 Gas -Phase Binding Studies

Electrospray ionization mass spectroscopy was also used to evaluate the alkali metal binding selectivities and complex stoichiometries of **4** and **5**. In the electrospray ionization method, complexes are formed in an appropriate solution and transported into the gas phase via a process in which they remain charged and are solvated.[28] The ions that are observed in the resulting mass spectra reflect the types and distributions of complexes initially present in solution. The electrospray ionization mass spectrometric method has been developed recently to estimate binding selectivities of host and binding constants of host-guest complexes based on measurement of the ion intensities of relevant complexes observed after spraying solutions containing well-defined compositions of host and guest species.[29] For the present study, solutions were prepared by mixing aliquots of chloroform containing the host at $5 \times 10^{-5}$ M and equal volumes of methanol solutions containing alkali metal salts at $5 \times 10^{-3}$ M. These mixtures having a final host: alkali metal 1: alkali metal 2 ratio of 1:100:100, were analyzed by an electrospray ionization quadrupole ion trap mass spectrometer. Examples of the mass spectra are shown in figure 3.6 for host **5** with $K^+$ and $Rb^+$, and $Rb^+$ and $Cs^+$. These types of mixtures produce clean and intense spectra that contained only 1:1 host:alkali metal complexes without interferences from

solvated complexes. Even at guest to host ratios of 100:1, the formation of 2:1 host: metal complexes are not observed, confirming that complexation of two metal ions by a single host does not occur. As shown in Figure 5, host **5** has a significant preference for complexation of $Rb^+$ over $K^+$ (Figure 3.6A) and an even greater affinity for $Cs^+$ over $Rb^+$ (Figure 3.6B).

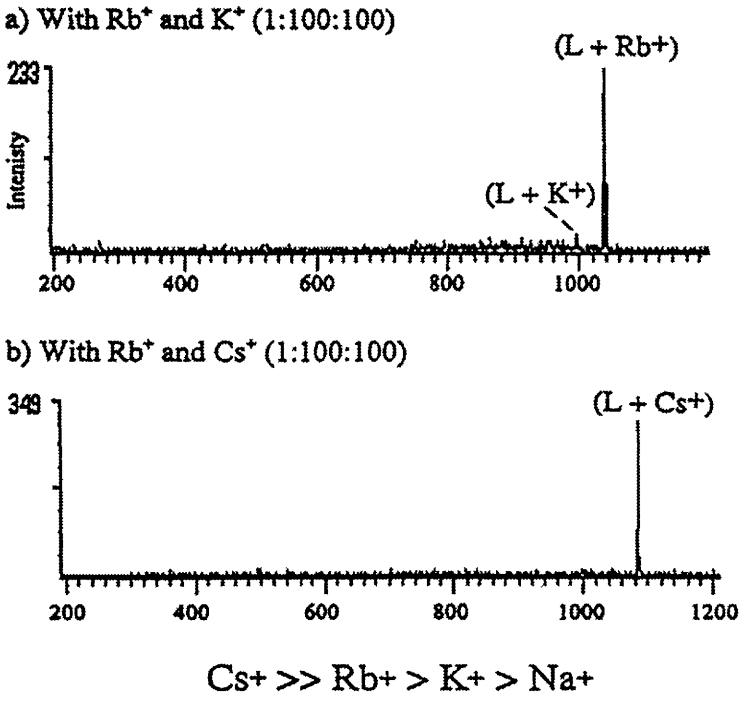


**Figure 3.6** *ES-MS Competition Mass Spectra for 5 with (a) $Rb^+/K^+$ and (b) $Cs^+/Rb^+$*

The results are similar for host **4** (data not shown), but careful measurement of the intensities of the complexes reveals that host **5**

demonstrates a higher degree of selectivity than that of **4**. The selectivity can be expressed as a ratio of the intensity (I) of one alkali metal complex to that of another, such as $I_{(host\ 4 + K^+)} / I_{(host\ 4 + Na^+)}$. For example, the $K^+/Na^+$ selectivity for host **4** is 11:1, whereas it is 20:1 for host **5**. Likewise, the $Rb^+/K^+$ selectivity for host **4** is 5:1, whereas it is 13:1 for host **5**. The $Cs^+/Rb^+$ selectivities were so large that they exceeded the dynamic range of the ion trap mass spectrometer (i.e. the intensities of the $Rb^+$ complexes were indiscernible from the baseline), thus preventing assignment of a finite ratio. To obtain a more quantitative estimation of the $Cs^+/Rb^+$ selectivity, solutions containing 1:10:10 and 1:1:1 ratios of host to $Rb^+$ to $Cs^+$ were sprayed in order to influence the equilibrium established in solution, but even at these reduced ratios the (host + $Cs^+$) complexes dominated the spectra. This great preference for $Cs^+$ complexation over a wide range of solution compositions suggest that the binding constants for the host:$Cs^+$ complexes are at least two orders of magnitude greater than those for the host:$Rb^+$ complexes in the chloroform/methanol solutions.

In addition to the overall greater selectivity of host **5** relative to host **4**, the intensities of the complexes containing host **5** were typically twice as great as those of host **4**. This result suggests that the binding constant of host **5** is greater than that of host **4**, in agreement with the results presented later in Table 1. Direct comparison of the binding affinities of host **4** and **5** by electrospray ionization mass spectrometric measurements of solutions containing both host with a single alkali metal could not be undertaken because these two host

posses the same molecular weight, thus prohibiting distinction of their complexes.

### 3.5 Picrate Extractions

Metal picrates have been utilized as molecular probes in the complexation of a number of cations with host in supramolecular chemistry. All bis-bridged compounds were dissolved in 2.0 mL of $CHCl_3$ at approximatly 1.0 mmol concentrations and shaken with equal molar amounts and volumes of aqueous metal picrate solutions.[21] The yellow colored metal picrates have a maximum absorbance at 354 nm in the UV region. The absorbance at 354 nm ($H_2O$) and 380 nm (CHCl3/Acetonitrile) was used to monitor the metal concentrations in either phase. Metal alkali picrates are easly obtained by the neutralization of trinitrophenol (picric acid) with the desired metal hydroxide of choice. Generally, excess base is used to assure no picric acid is present during extractions. Another method involves the isolation of the salt by recrystallizing an equal molar solution of picric acid and corresponding metal hydroxide in water and ethanol (1:1). This procedure is undesirable due to the explosive potential of picric acid and even greater instability of the metal picrate salts, mainly when the salts are completely dry. Utmost care and precautions were taken in handling and storing the picrates, and no complications were encountered. The concentration of the bis-crowns (**4** and **5**) in the extraction experiments were all prepared to an approximate equal molar concentration to the aqueous metal picrate solutions.

The binding (Ka) and extraction (Ke) constants of metal picrate salts complexes with **4** and **5** demonstrated that both conformers display a high selectivity for the larger rubidium and cesium ions (Table 3.1). For example, the cone conformer **5** extracted 51% of the cesium picrate from a 9.2 x $10^{-4}$ M aqueous solution into the chloroform solution of the host at a 1:1 (host to guest) ratio, but extracted only 3% of the $Rb^+$ salt and almost none of the smaller $Li^+$, $Na^+$, and $K^+$ salts.

**Table 3.1** *$K_e$ and $K_a$ values for host **4** and **5**.*

| | Cone **5** | | 1,2,3-Alternate **4** | |
|---|---|---|---|---|
| Metal picrate | $K_e$ x $10^{-3}$ M | $K_a$ x $10^{-5}$ $M^{-1}$ | $K_e$ x $10^{-3}$ M | $K_a$ x $10^{-5}$ $M^{-1}$ |
| $Li^+$ | 4300 | 8000 | 210 | 390 |
| $Na^+$ | 37 | 810 | 7.1 | 15.5 |
| $K^+$ | 5.3 | 21 | 0.7 | 2.7 |
| $Rb^+$ | 0.9 | 5.2 | 0.3 | 1.2 |
| $Cs^+$ | 1.2 | 8.4 | 0.5 | 3.5 |

The results of extraction studies conducted on bis-crowns **4** and **5** are summarized in Table 3.1. The $K_e$ and $K_a$ values reinforced the premise derived from the NMR studies that both hosts have high affinities for $Cs^+$ and $Rb^+$ over $K^+$, $Na^+$, $Li^+$. The cone isomer **5** bound cesium approximately ten times better than rubidium, but about 400 times better than potassium and 1500 times better than sodium or lithium. In past research, it was shown that a rigid preorganized bis-crown-3-calix[8]arene bound a cesium over sodium cation 1400 times better, comparible to our selectivity value for **5** (see Figure 3.7).[30]

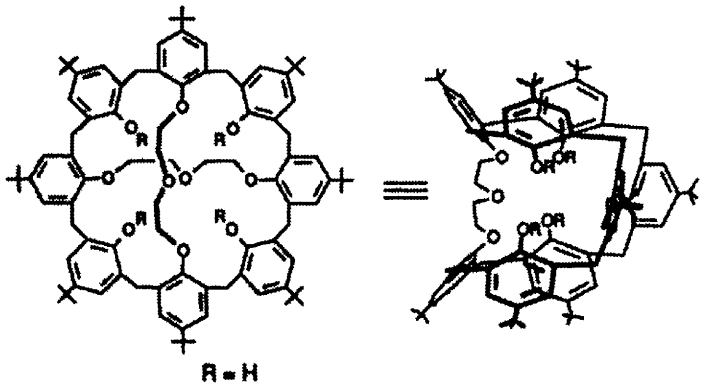


**Figure 3.7** *Bis-crown-3-calix[8]arene showing similar $Cs^+/Na^+$ selectivity to* ***5***

An example where a calix[4]arene-crown-6 has an especially high $Cs^+/Na^+$ selectivity factor of *ca.* 4000 is shown in Figure 3.8. The conformationally mobile calixarene takes advantage of the cation-π interaction by adopting a 1,3-alternate conformation.

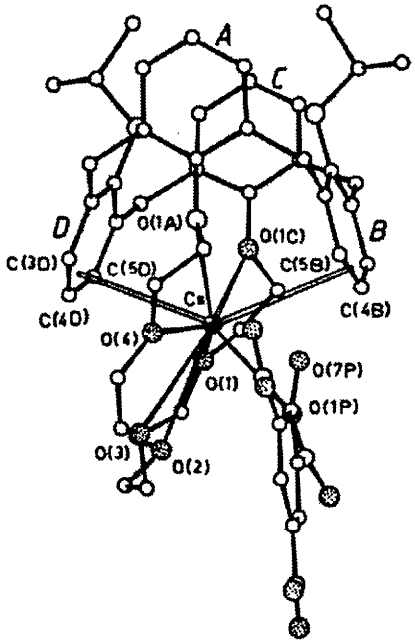


**Figure 3.8** *A 1,3-Alternate Conformer of Calix[4]arene-crown-6 with high $Cs^+/Na^+$ selectivity*

The $Cs^+$-$\pi$, metal to centroid distances are approximately 0.2 Å shorter than distances calculated in the $Cs^+$-**5** complex.

The 1,2,3-alternate conformer exhibited the same selectivity trend but the selectivity ratios are not quite as high. For example, **4** bound cesium roughly 25 times tighter than it did rubidium and only 144 times better than the smaller cations. Another general trend is that the cone isomer **5** binds cesium and rubidium ions about an order of magnitude better than **4**, but both bind the smaller cations equally well. The cone isomer has a large bowl shape which is lined with eight convergent oxygen atoms while the oxygen atoms in the 1,2,3-alternate isomer are in a 30-membered macrocyclic structure and held far apart. In comparison to other cesium-selective calixcrown-6 compounds, the $K_{ass}$ of the bis-crown cone isomer **5** is similar and towards the higher end while **4** is towards the lower.[3]

# 4.0 Results and Discussion of Bis-Aromatic Bridged Calix[6]arenes 6 and 7

## 4.1 Conformational analysis of bis -m-xylenyl calix[6]arene (6)

### 4.1.1 Solid State Data

The x-ray crystal structure for **6** clearly established that the calixarene framework is in a distorted 1,2,3-alternate conformation described by the chemical notation (u,uo,do,di,do,uo) with respect to the A allyl containing ring.

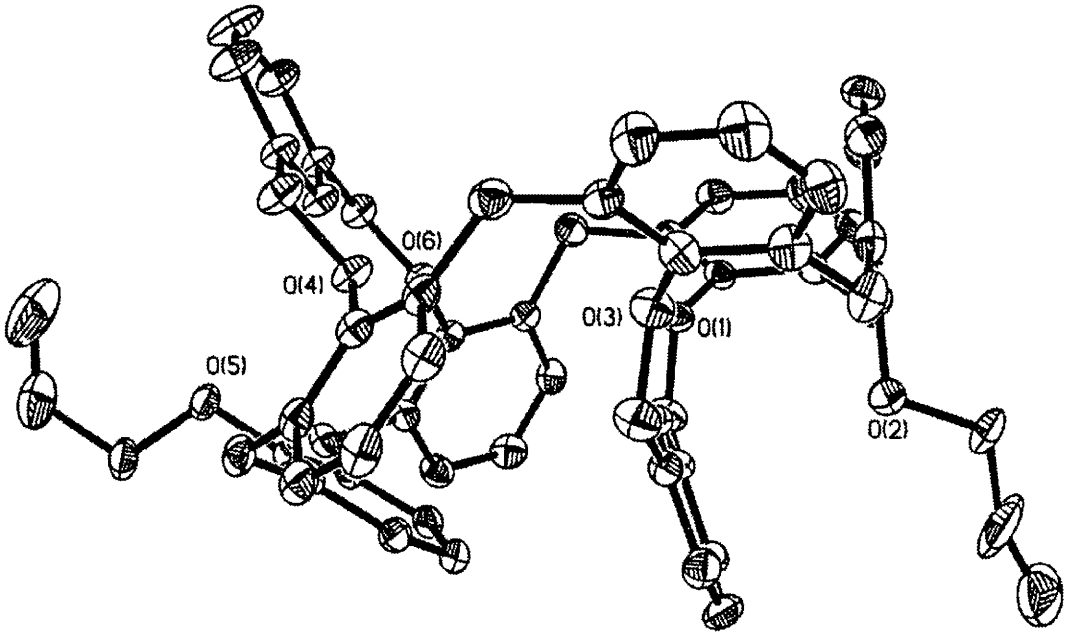


**Figure 4.1** *Ortep plot of **6** in a 1,2,3-alternate conformation.*

The $^{1}H$ and $^{13}C$ NMR spectra at low temperature (-80 °C) are analogous to the solid state crystal structure in that separate peaks were obtained for the two distinct halves of the molecule (Figure 4.4c). With only a vertical mirror plane

bisecting the A and D rings, the solid state structure of **6** has $C_2$ symmetry that renders the left and right halves equivalent but the top and bottom halves non-equivalent (Figure 4.2).

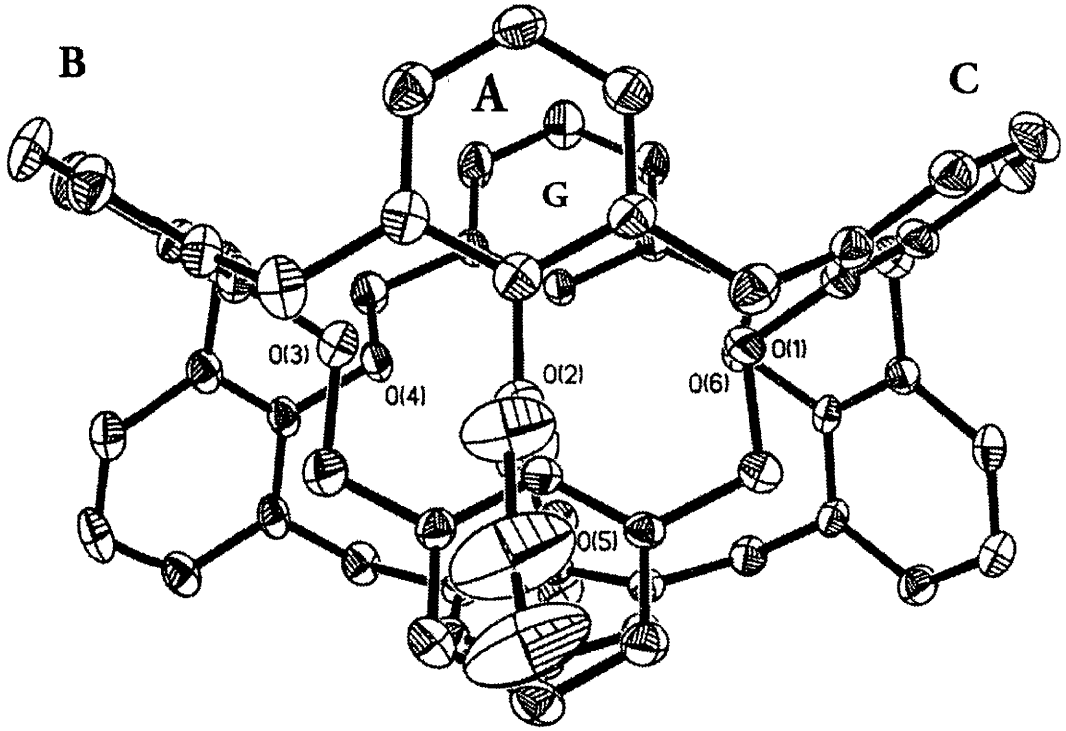


**Figure 4.2** *$C_2$ symmetry of Compound **6**.*

A calix[4]arene-like structure was created by the A, B and C rings of the calix and the xylene ring G at the top half of the molecule. The transannular distances across the top half are 8.89 Å (C5-C57) between the para carbon on ring B and the distal carbon on the xylenyl strap and 11.16 Å (C11-C35) for the para carbons on rings A and C giving the structural characteristic of a calix[4]arene while having the dimensions of a calix[6]arene.[2] The bottom half is defined by rings D, E, F and the corresponding xylenyl H ring where the rings D and F are

similar in distance as the top half but the distance between (C23-C46) is only 3.81 Å(Figure 4.3).

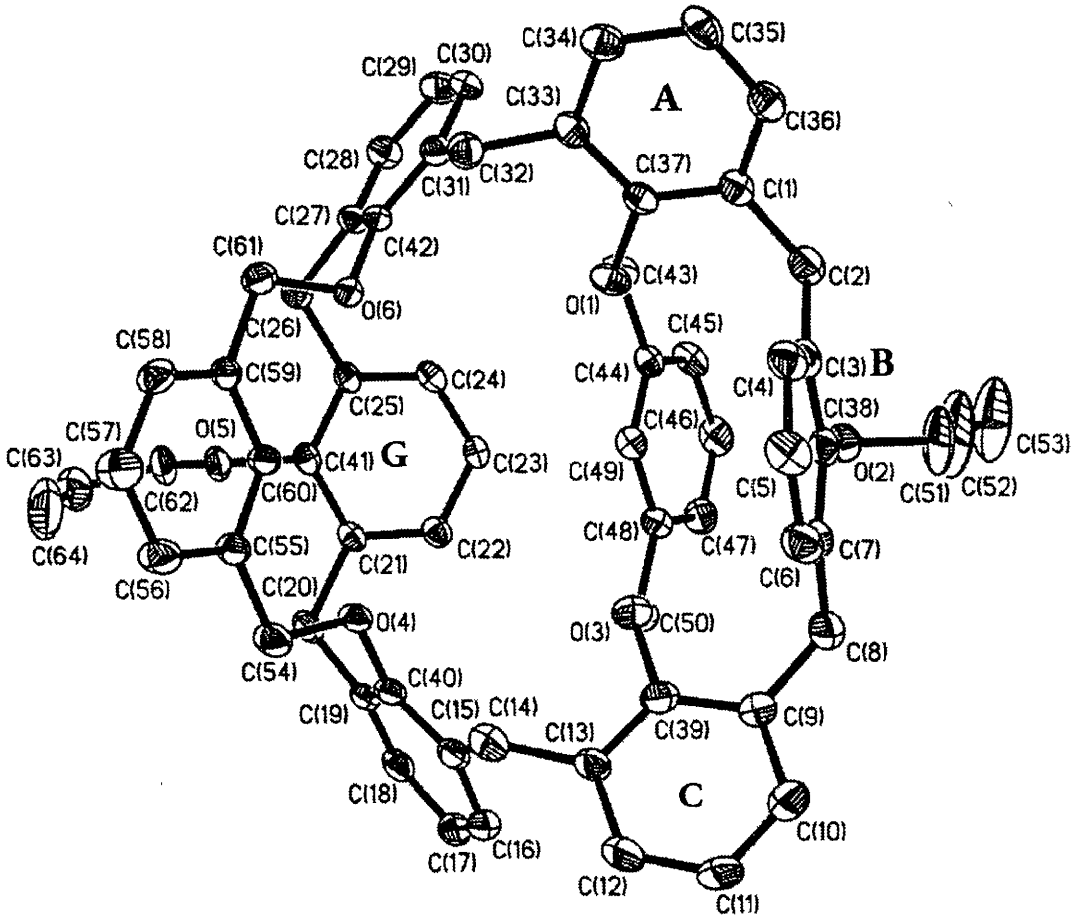


**Figure 4.3** *Top view of compound **6**.*

### 4.1.2 Solution State Data (6)

The $^1$H NMR spectrum of **6** displayed considerably broadened signals at 25 ˚C for the $ArCH_2Ar$ and $ArCH_2O$ protons which indicated conformational mobility leading to difficulties in its initial interpretation (Figure 4.4b). However all of the coalesced signals were accounted for by using variable temperature one-

and two-dimensional NMR spectroscopy ($^{1}H$, $^{13}C$, $^{1}H/^{1}H$ COSY, $^{1}H/^{13}C$ HETCOR see Appendix 9-12).

When a $CDCl_3$ solution of **6** was cooled to -80 °C in THF-$d_8$, most of the signals split with one set of signals arising from the F, A, and B rings and a shifted set of signals for the C, D, and E rings.

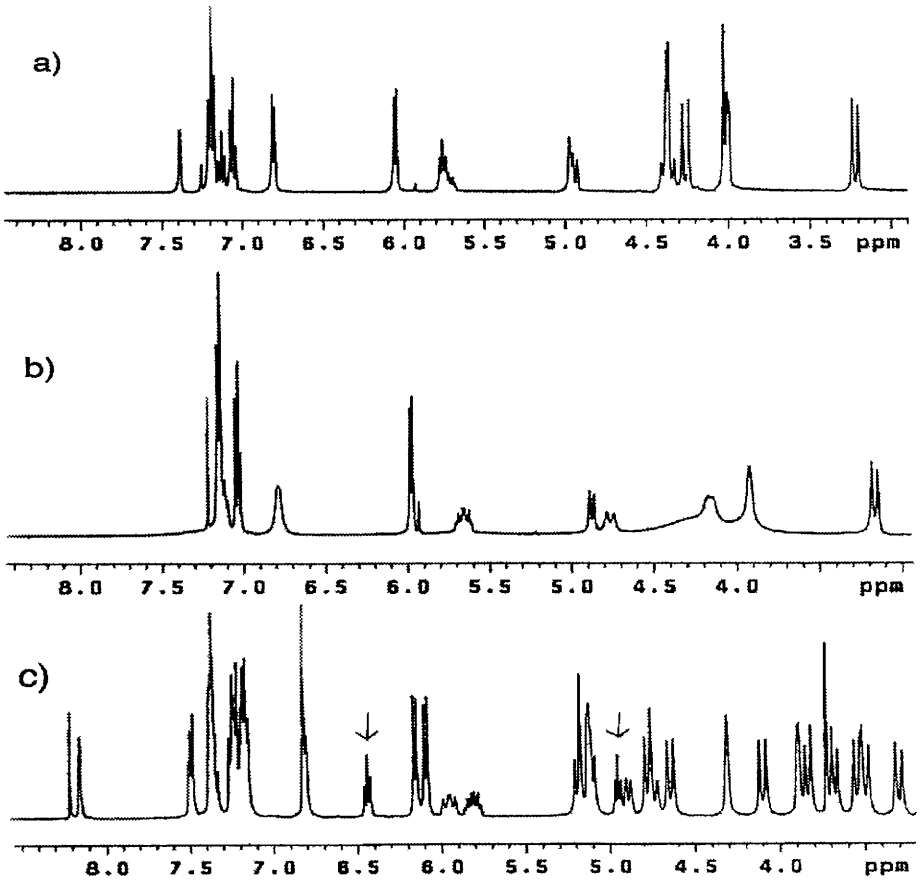


**Figure 4.4** *$^{1}H$-NMR spectra for compound **6** at (a) 140 °C, (b) 25 °C, (c) -80 °C*

The para hydrogens of the allyl containing rings (A,D) experience dramatically different environments at -80 °C. The chemical shift for the para hydrogen on the A ring is deshielded to 6.44 ppm, while the same hydrogen on

the inverted D ring is shielded to 4.95 ppm due to its closer proximity to the $\pi$ cloud of the bridging xylene ring H. The $^{13}$C-NMR spectrum contained a total of 39 signals in which three $ArCH_2Ar$ signals appear at 31.02, 31.21, 31.85 ppm

The compound undergoes conformational equilibration and the spectrum adopts a degenerate set of signals for one half of the symmetrical compound at 140˚C in $C_2D_2Cl_4$. The $ArCH_2Ar$ hydrogens attached to the two anti-oriented carbons (C14, C32) appeared as a singlet while those bonded to the syn-oriented carbons (C2, C8, C20, C26) appeared as an AB-quartet. The para hydrogens on the B and E rings appear as one triplet at 5.73 ppm. And the 19 $^{13}$C signals indicate rapid equilibration of rings A and D as a result of the $C_2$ and i symmetry elements. The $^{13}$C NMR spectrum shows two $ArCH_2Ar$ signals at 30.86 ppm for the two anti $ArCH_2Ar$ and 31.28 ppm for the four syn oriented $ArCH_2Ar$ carbons. The chemical shift of the $ArCH_2Ar$ carbons between the anti-oriented rings are shielded to higher fields than expected (approximately 6 ppm) while the signal for the syn oriented $ArCH_2Ar$ has a "normal" chemical shift. This again is another contradiction to the conformational $^{13}$C-NMR rule.[11]

## 4.2 Conformational Analysis of 7

### 4.2.1 Solid State Data of 7 (cesium complex)

The x-ray crystal data was incomplete and the crystal structure was not fully solved, however it is useful to aid in the conformational analysis of the cesium complex.

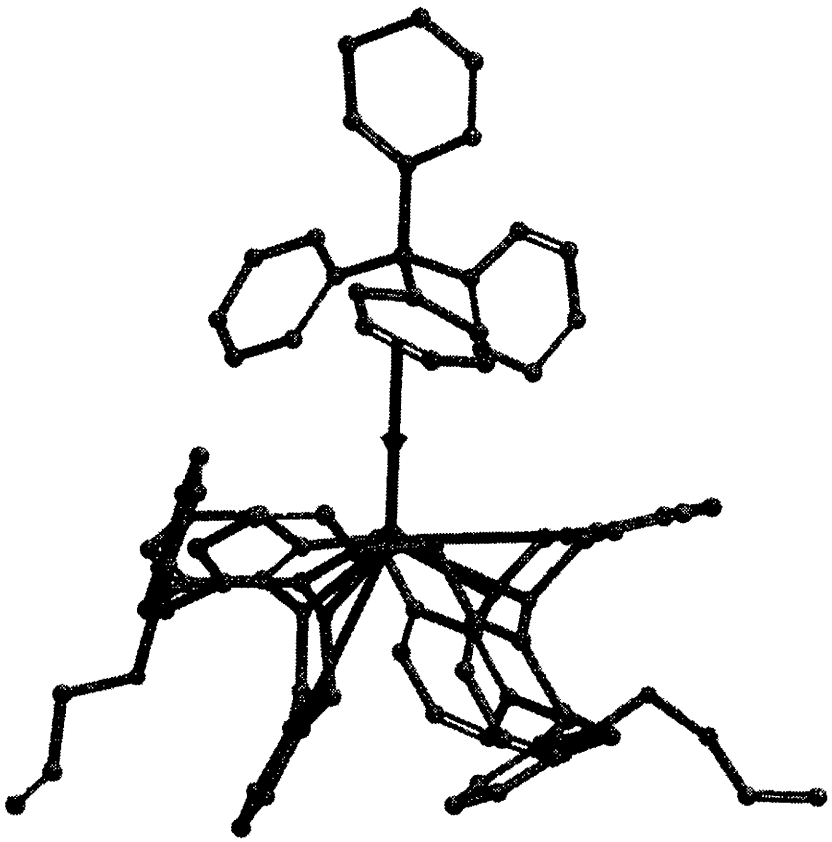

**Figure 4.5** *Partially resolved crystal strucure of* ***7*** *- $Cs^+$ complex*

Due to the presence of two pyridinyl straps, 1:2 (host-guest) complexes could have been possible, nevertheless **7** actually harbors a single metal ion in the

center of the calixarene. Furthermore, there is an $\eta^2$, $\pi$-metal interaction with the cesium ion and one of the phenyl rings of the tetraphenylborate counter ion (Figure 4.5).

### 4.2.2 Solution State Data (7)

In contrast to the $^1$H-NMR spectra for **6**, compound **7** has no broadened signals and designation of signals can be determine at room temperature. The top and bottom halves are seen as one set of degenerate signals in rapid exchange. Upon the addition of alkali metal picrates to a solution of **7** in $CDCl_3$ similar NMR spectra resulted in that when complexed the top and bottom halves are in slow exchange, analogous to the low temperature NMR spectra of **6**. Fast exchange of the top and bottom halves occur over a temperature range of -85 ˚C to 100 ˚C where very little change is seen in the NMR spectra. Due to rigidity and rotational hindrance, all of the $ArCH_2Ar$ hydrogens are diastereotopic. The $ArCH_2Ar$ hydrogens linking the aromatics of the calixarene framework appeared as a singlet at 4.24 ppm for the four anti-hydrogens and a pair of doublets at 4.11 and 3.16 ppm for the eight syn hydrogens. The $ArCH_2Ar$ hydrogens on the pyridinyl straps appeared as a pair of doublets at 4.56 and 4.16 ppm. The $^{13}$C NMR spectrum at room temperature showed 19 carbon signals, indicative of equivalent symmetrical halves as a result of $C_2v$ symetry. The syn and anti carbons at 31.03 and 30.78 ppm, respectively, have a $\Delta\delta$ = .75 ppm. Once again, this is value

contradictory to the conformational diagnostic tool proposed by Gutsche, which would erroneously predict that **7** existed in the cone conformation.[11]

### 4.3 NMR Metal Complexation Analysis via NMR titration of 7

#### 4.3.1 NMR $Rb^+$ Titration with 7

The rate of exchange between the free and complexed host was slow on NMR time scale at room temperature for **7,** when complexed with alkali metals. Compound **7**, had a high affinity for all of the metals tested which resulted in nearly complete, separate peaks from the unbound host in slow exchange. Total complexation of **7** is achieved at 1:1 mole ratios of host-guest; in fact less, than 1 molar equivalent must be used to observe both complexed and free host signals simultaneously (Figure 4.6).

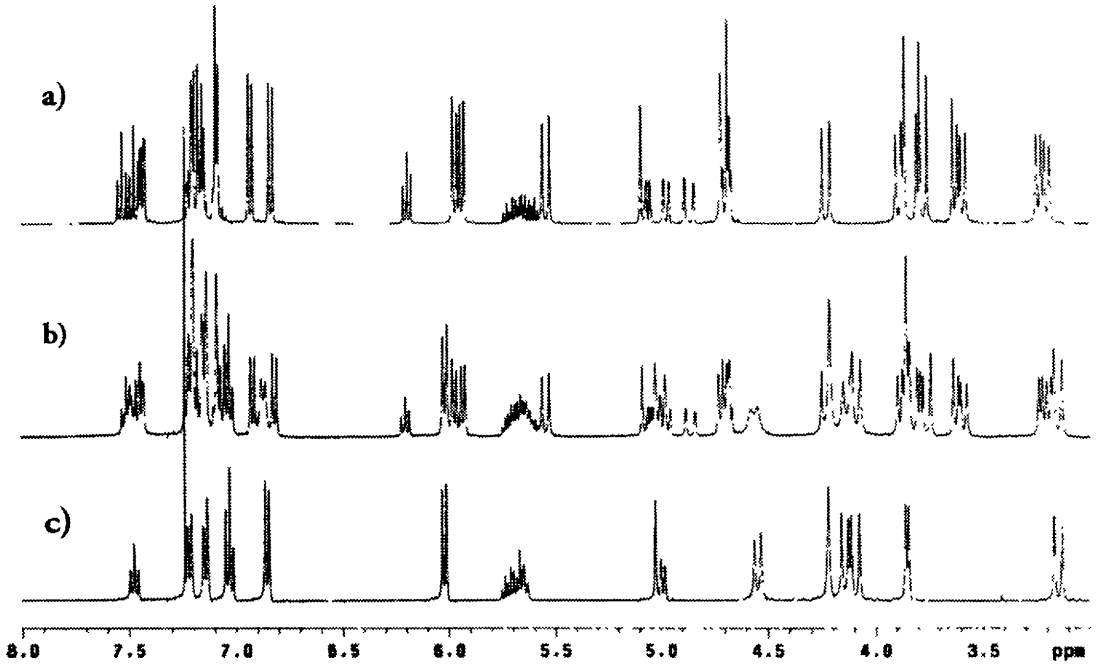


**Figure 4.6** *$^1$H-NMR of compound **7** with a) 1.0, b) 0.5 and c) 0.0 molar equivalent of $Rb^+$.*

### 4.3.2 $^1$H-NMR Spectra of 7-Alkali Metal Complexes

When compound **7** was complexed with different sized alkali metals, unique $^1$H-NMR spectra resulted (Figure 4.7).

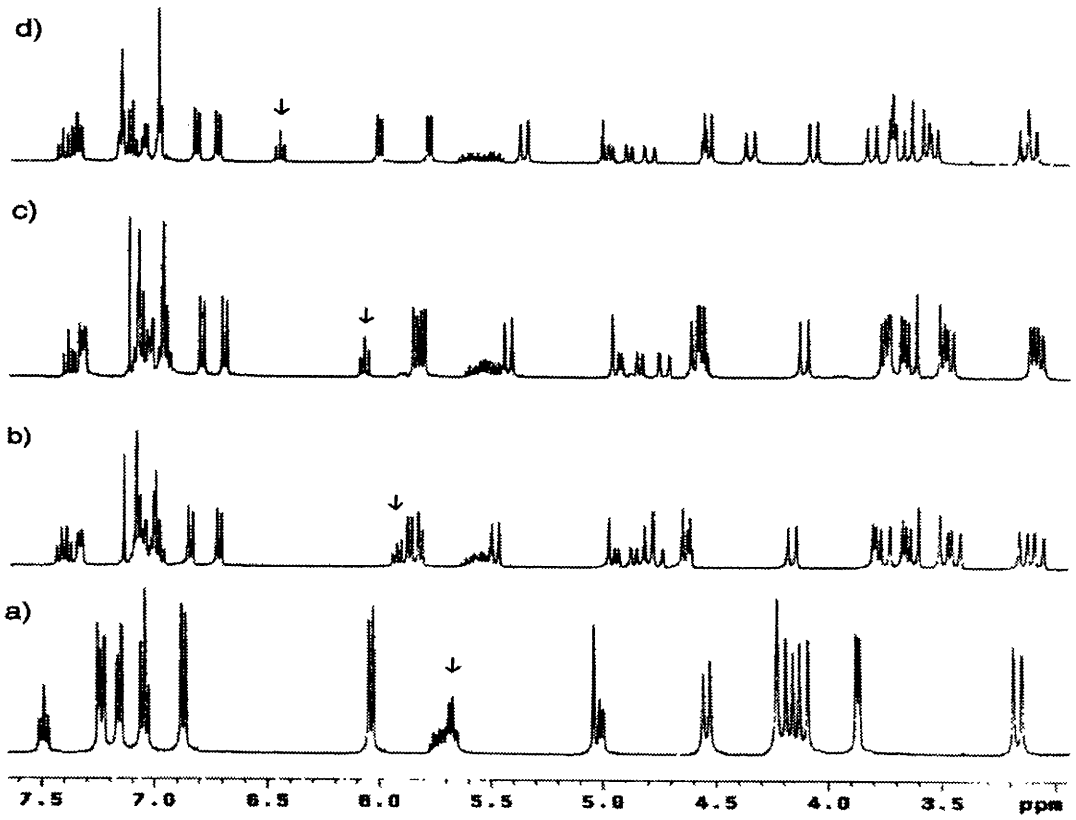


**Figure 4.7** *Stack plot of compound **7** with a) $Cs^+$, b) $Rb^+$, c) $K^+$, and d) Free host*

The most dramatic change occurred in the triplet representing the para hydrogens of the allyloxy aromatic rings which occurred at 5.67 ppm for the uncomplexed host. The para hydrogen on the allyloxy aromatic closest to one of the pyridinyl rings (see Figure 4.5) was shielded up field between (4.6 - 4.8 ppm)

and remained relatively stationary throughout the alkali series. The other proton was shifted further down field with each consecutive larger alkali metal complex, ending with cesium at 6.49 ppm (Figure 4.7). One explanation is that when larger cations were complexed the top pyridinyl ring (Figure 4.5) is pushed further away from the proton on the alkylated ring which reduced the shielding effect.

### 4.4 Free Energies of Conformational flexibility of 6 and Decomplexation of the $Rb^+$-7 complex

The free energy of activation for decomplexation was measured by variable temperature $^1$H-NMR using the equation below.

$$\Delta G^{\ddagger}_{Tc^{\circ}K} = 19.14[T_c(9.97 + \log T_c/\Delta\nu)]$$

$T_c$ is the temperature of coalescence and $\Delta\nu$ is the difference in chemical shift between the two states below coalescence.

The value calculated for the free energy of activation required to induce flexibility of **6** was ($\Delta G^{\ddagger}_{263\ ^{\circ}K}$= 52 kcal/ mole) from the coalesced spectra at -15 °C.[31] The spectra at coalescence, takes on extreme broadness.

Decomplexation of **7** with $Rb^+Pic^-$ was obtained by $^1$H NMR by incrementally increasing the temperature until coalescence was obtained indicating decomplexatation of $Rb^+$ had taken place. The temperature of coalescence was 80°C and the $\Delta G^{\ddagger}_{353\ ^{\circ}K}$ for decomplexation is 80 kcal/mol.

### 4.5 Metal Picrate Extractions

The bis aromatic bridged compounds varied considerably in binding behavior from one another. Compound **6** had almost no binding capability in near equal molar (host:guest) concentrations ($1.0 \times 10^{-3}$ M) while **7** gave high extraction constants for all of the alkali metal salts. For **6,** host concentrations were increased 5 and 10 fold yet no extraction took place as evident by the concentration of metal picrate in the aqueous phase remaining unchanged, and the picrate concentration in the $CHCl_3$ layer lying below the limit of detection for our instruments.

Extractions done with host **7** and equal molar amounts of all picrate salts completely stripped the aqueous layer containing the picrates, below the UV detection limit. The host concentration of **7** was halved so Ke values could be obtained.[21]

**Table 4.1** *$K_a$, $K_e$ and $K_d$ values for compound 7.*

| Metal picrate | $K_e \times 10^{-3}$ $M^{-1}$ | Ka x $10^{-6}$ $M^{-1}$ | $K_d \times 10^3$ ,$M^{-1}$ |
|---|---|---|---|
| $Li^+$ | 2.55 | 1.8 | 1.42 |
| $Na^+$ | 7.74 | 4.44 | 1.74 |
| $K^+$ | 18.7 | 7.32 | 2.55 |
| $Rb^+$ | 277 | 60.7 | 4.57 |
| $Cs^+$ | 18.5 | 3.43 | 5.41 |

A control was tested using picric acid instead of the metal picrate salts in an extraction with **7**. The control experiment also resulted in a high extraction percentage. Interestingly the $^1$H-NMR of host **7** with picric acid showed broad

signals throughout the entire spectra most likely resulting from acid protonation of the pyridinyl nitrogen(s). Other evidence was the unique chemical shifts of protons on the NMR spectra for all of the bound picrate metals. To assure acid/base effects did not interfere with results of the metal picrate extraction binding, the bispyridinyl compound was washed with 1 N NaOH to ensure that the nitrogens atoms were not protonated. Although host **7** extracted all of the metal picrates strongly, there is a slight preference for $K^+$ followed by $Rb^+$, $Cs^+$, $Na^+$ and $Li^+$. The extraction studies of the two host compounds **6** and **7** showed that extraction behaviors were dramatically different.

# 5.0 Experimental

See appendix for additional NMR spectra

## 5.1 Materials

Tetrahydrofuran (THF) was freshly distilled from sodium/ benzophenone or used directly out of a sure sealed bottle, all other solvents were used as is with the exception of the preparation of the chloroform solution used in the picrate extraction experiments. All the other reagents were purchased through Aldrich, and used without further purification. $^{1}$H-NMR and $^{13}$C-NMR data was collected on a 400 MHz Varian NMR. Chemical shifts ($\delta$) are expressed in ppm relative to the internal tetramethyl silane (TMS). All melting points were obtained in unsealed capillary tubes and are uncorrected. Elemental analyses were performed at Desert Analytics Laboratory in Tucson, Arizona. All reactions were carried out in a dry argon atmosphere. Analytical TLC was performed on precoated silica gel plates (Silica Gel IB2-F) and column chromatography was performed with Silica Gel 1B2-F 150, 60-200 Mesh (75-250 micron).

## 5.2 Preparation of 5, 11, 17, 23, 29, 35-hexa-*p-tert*-butyl-37,38,39,40,41,42-hexahydroxycalix[6]arene (1)

To a 3 liter three necked, round-bottom flask equipped with a mechanical overhead stirrer, Dean-Stark trap, and condenser, 100.0 g, (0.666 mol) of 4-*tert*-butyl phenol and 40.0 g of paraformaldehyde were suspended in 1.5 liters of xylene. To the suspension 26.65 mL, (exactly 0.34 molar equivalents .2363 mol)

of rubidium hydroxide in a 50% wt. aqueous solution, was delivered via 25 mL volumetric pipette and adjustable micropipettes. A Dean-Stark trap was filled with xylene and the reaction was allowed to reflux under an argon atmosphere. During the initial hour of the reaction, the temperature was increased to reflux. The suspension dissolved and the reaction mixture and appeared clear yellow and progressed to a dark coffee color where the tan crude product precipitated. After 20 h the reaction was allowed to cool and filtered through a Buchner funnel leaving a solvent soaked plug with a consistency of a wet dirt/clay. The filter cake was then dissolved in $CHCl_3$ (2 L) and washed 3 X with 1M HCl (1.5 L) and once with brine, an aqueous solution saturated with NaCl, (1.5 L). Severe emulsion arose during the washes. Emulsions were allowed to settle over a period of days and back extractions were preformed on the aqueous layer. All of the $CHCl_3$ washes and back extractions were combined and dried over $MgSO_4$ and filtered. The solvent was reduced to 200 mL and recrystallized with $CH_3OH$ or the compound eventually crystallized in $CHCl_3$. The slightly off white crystalline powder precipitate was filtered yielding 82 g (76%). mp. 380-381˚C; R*f* = .63 in $CHCl_3$ (3 parts)/hexane (4 parts); $^1H$ NMR (400 MHz, $CD_2Cl_2$) $\delta$ = 10.2 (s, ArOH 12H), 7.10 (s, ArH, 12H), 3.88 (s, $ArCH_2Ar$, 12H), 1.25 (s, $C(CH_3)_3$, 54H). $^{13}C$ NMR (400 MHz, $CHCl_3$) $\delta$ = 147.2, 144.2, 126.9, 126.1, 34.0, 33.1, 31.4.

**5.3 Preparation of 37,38,39,40,41,42-hexahydroxy Calix[6]arene (2)**

To a flame dried 3 liter three necked, round-bottom flask equipped with a mechanical overhead stirrer, 70.0 g (.072 mol) of compound **1** along with 60 g (.65 mol) of phenol and 115 g (.863 mol) of $AlCl_3$were dissolved in 1.5 L of toluene. The reaction was allowed to stir for 48 h at which time 1 L of 0.1 N HCl was added to quench the reaction. The organic layer was separated and the toluene was removed under reduced pressure. The residue was redissolved in 1.5 L of $CHCl_3$ and washed 2 X with 0.1 M HCl (1.5 L) and once with brine. The organic layer was then dried over $MgSO_4$ and filtered. The solvent was evaporated under reduced pressure to almost dryness.The crude product was poured into approximately 1.5 L of methanol with stirring. Compound **2** precipitate from solution. The white solid was filtered to provide 39.1 g (85%) mp. 417-418˚C $^1H$ NMR (400 MHz, $CDCl_3$) $\delta$ =10.4 (s, 6H, ArOH), 6.7-7.4 (m, 16H, ArH), 4.0 ( s, 12H, $ArCH_2Ar$)

**5.4 Preparation of 37,40-Diallyloxy-38,39,41,42-tetrahydroxycalix[6]arene (3)**

To a flame dried 2.0 L two necked, round bottom flask with a magnetic stir bar 20.0 g (32.7 mmol) of compound **2** and 27.1 g (190 mmol) of potassium trimethyl-silanolate $K^+(CH_3)_3SiO^-$ was placed in 1.20 L of freshly distiled THF and 120 mL of DMF. After the reaction was cooled for 15 min in a 0 ˚C ice bath, 7.75 mL (88.7 mmol) of allylbromide was added and the reaction was allowed to stir for 3 h. The reaction solvent was removed under reduced pressure using a water

aspirator to remove most of the THF and then switching to a mechanical vacuum pump to remove the remaining DMF solvent. The residue was then taken up in $CHCl_3$ (1 L) and washed 3 X with equal volumes (1 L) of 1 M HCl followed by a brine wash. The solution was then dried over $MgSO_4$, filtered, and the volume was reduced to approximately 100 mL and poured into 800 mL of hexane. The solution was filtered to obtain the product in high yields 21.8 g (96%). mp 188-190 °C. $^1$H NMR (400 MHz, $CDCl_3$) δ = 8.03 (s, 4H, -OH), 7.09-6.89 (m, 14H, ArH), 6.76 (t, 4H, ArH, J=6.0 Hz), 5.95 (m, 2H, -CH=), 5.40 (d, 2H, =CH2, J= 20.0 Hz), 5.08 (d, 2H, $=CH_2$, J=12.0 Hz), 4.46 (d, 4H, $-OCH_2-$, J=6.0 Hz), 3.94 and 3.78 (two s, 12H, $ArCH_2Ar$). $^{13}$C NMR (400 MHz, $CHCl_3$) δ = 162.5, 152.4, 151.8, 133.2, 131.8, 129.1, 128.9, 128.7, 127.5, 127.1, 125.5, 120.2 and 118.5 (Ar and $-CH=CH_2$), 75.9 ($-OCH_2-$), 36.4 and 31.5 ($ArCH_2Ar$).

**5.5 37,40-Diallyloxy-(38-42),(39-40)-biscrown[4]ether-calix[6]arene (4 and 5)**

In a 500 mL round-bottom flask, 2.0 g (2.8 mmol) of compound **3** and 0.68 g (16.9 mmol) of NaH was dissolved in 200 mL of THF/DMF (10:1) and the solution was stirred for 30 min at room temperature. Triethylene glycol di-*p*-tosylate (3.2 g, 6.8 mmol) dissolved in 50 mL of THF was added via addition funnel and the reaction was heated to reflux for 24h. The solvent was removed under reduced pressure and the residue was redissolved in $CHCl_3$ (100 mL) and washed with equal volumes of 1N HCl (3X) and brine (1X). The organic solution

was dried over $MgSO_4$, filtered and concentrated. Separation of **4** and **5** was achieved by column chromatography on silica gel (90% $CHCl_3$/10% EtOAc).

**1,2,3-Alternate Isomer (4).** 0.4g (15 %), Rf = 0.73, mp = 235-240 ˚C $^1$H-NMR (400 MHz, $CDCl_3$) δ = 7.18-7.15 (d of d, J = 7.2 Hz, 4H), 7.13-7.11 (d of d, J = 7.6 Hz, 4H), 6.99 (t, J = 7.6 Hz, 4H), 6.66 (t, J = 8.0 Hz, 2H), 6.51 (d, J = 7.6 Hz, 4H), 6.19-6.13 (m, 2H), 5.41 (d, J = 16.0 Hz, 2H), 5.23 (d, J = 10.4 Hz, 2H), 4.55 (d, J = 15.2 Hz, 4H), 4.36 (d, J = 5.6Hz, 4H), 3.99 (s, 4H), 3.54-3.38 ( m, 16H), 3.24 (m, 4H), 3.11 (m, 4H), 3.03 (m, 4H). $^{13}$C NMR (400 MHz, $CDCl_3$), δ = 156.47, 154.33, 134.70, 134.39, 133.97, 133.48, 130.17, 129.66, 136.66, 123.69, 123.37, 117.52, 74.43, 72.57, 70.78, 69.98, 31.61, 31.28. Elemental anal. calcd. for $C_{60}H_{64}O_{10}$ %C: 76.25, %H: 6.83. Found: %C 76.49, %H 6.92.

**Cone Isomer (5).** 0.3g (11 %), Rf = 0.60, mp = 230-232 ˚C $^1$H NMR (400 MHz, $CDCl_3$) d 7.58-7.56 (d of d, J = 6.8 Hz, 4H), 7.12-7.06 (d of t, J = 8H), 6.29 (t, J = 7.6 Hz, 2H), 6.17 (m, 2H), 6.03 (d, J = 7.6 Hz, 4H), 5.65-5.61 (d of d, J = 17.2 Hz, 2H), 5.30-5.27 (d of d, J = 10.4 Hz, 2H), 4.61 (d, J = 16.4 Hz, 4H), 4.59 (d, J = 13.2 Hz, 2H), 4.51 (d, J = 3.6 Hz, 4H), 4.02 (d, J = 9.0 Hz, 4H), 3.85-3.72 (m, 12H), 3.54 (d, J = 13.6 Hz, 4H), 3.46-3.43 (m, 6H), 3.13 (d, J = 10.8 Hz, 4H). $^{13}$C-NMR (400 MHz, $CDCl_3$) δ = 155.63, 154.21, 135.09, 134.29, 134.20, 133.25, 130.63, 129.46, 125.99, 123.76, 122.94, 116.29, 73.54, 72.52, 71.43, 70.66, 30.88, 27.09. Elemental anal. calcd. for $C_{60}H_{64}O_{10}$ %C: 76.25, %H: 6.83. Found: %C 76.66, %H 6.87.

**5.6 27'40-Diallyloxy-(38,41)-(39,42)-bis-m-xylenyloxycalix[6]arene (6)**

In a 500 mL single necked round bottom flask 2.0 g (2.8 mmol) of compound **3** dissolved in a 200 ml of THF containing 20 ml of DMF .68 g (17 mmol) of a 60% NaH dispersion in mineral oil and allowed to stir at room temperature for 30 min before 3.8 g (14 mmol) of α,α-di-bromomethyl-*m*-xylene was added. The solution was refluxed for 24 h at which time the solvent was removed under reduced pressure. The residue was dissolved in $CHCl_3$ (100mL) and wash 3x with 1 N HCl followed by a brine wash and dried over $MgSO_4$. The solvent was reduced and the crude product was purified by column chromatography on silica gel 70% $CH_2Cl_2$ 30% Hex (Rf = .85) yields 65% (1.6 g) m.p. 261 – 263 ˚C (dec) $^1$H-NMR (400 MHz, $C_2D_2Cl_4$, + 140 ˚C) (δ = 7.39, s, (2H), 7.19, d of d, (8H), 7.13, t (j = 7.6 Hz), 7.06, t (j = 7.6 Hz), (4H), 6.80, d (J = 7.6 Hz), (4H), 6.06, d (J = 7.6 Hz), (4H), 5.76, t(J = 6.4 Hz), (2H), 5.73, m, (2H), 4.45, m, (4H), 4.39, d, (J= 12.8 Hz), (4H), 4.33, d, (j = 12.8 Hz), (4H), 4.25, d, (J = 15.2 Hz), (4H), 4.01, s, (4H), 3.99, d (J = 2 Hz), (4H), 3.21, d, (j = 15.2 Hz), (4H). $^{13}$C-NMR (400 MHz, $C_2D_2Cl_4$, + 140 ˚C) δ = 157.22, 153.62, 139.21, 136.32, 135.44, 134.30, 133.52, 130.74, 129.62, 126.46, 126.00, 124.69, 123.39, 123.19, 122.59, 115.54, 74.34, 73.49, 31.38, 30.86. Anal. Calcd for $C_{64}H_{56}0_6$: C, 83.5%; H, 6.1%; O, 10.4%.

**5.7 27'40-Diallyloxy-(38,41)-(39,42)-bis-(2,6-dimethylpyridinyloxy) calix[6]arene (7)**

In a 500 mL single necked round bottom flask 2.0 g (2.8 mmol) of compound **3** dissolved in a 200 ml of THF containing 20 ml of DMF and .68 g (17 mmol) of a 60% NaH dispersion in mineral oil was allowed to stir at room temperature for 30 min. Next 1.68 g (6.3 mmol) 2,6-bis(bromomethyl) pyridine was added and the solution was stirred for 5 days at which time the solvent was removed under reduced pressure. The residue was dissolved in $CHCl_3$ (100mL) and wash 3x with 1 N HCl followed by a brine wash and dried over $MgSO_4$. The solvent was reduced and the crude product was purified by column chromatography on aluminum oxide 60% EtOAc : 40% $CHCl_3$ (Rf = .65) yields 55% (1.4 g) m.p. 248 - 250.˚C $^1$H-NMR (400 MHz, $C_2D_2Cl_4$, + 140 ˚C) $\delta$ = 7.48, t, (J = 7.6 Hz), (2H), 7.23, d, (J= 8Hz), (4H), 7.15, d, (J = 7.6 Hz), (4H), 7.04, t, (J = 7.2 Hz), (4H), 6.86, d, (J = 7.2 Hz), (4H), 6.03, d, (J = 8 Hz), (4H), 5.72, m, (2H), 5.57, d, (J = 7.2 Hz), (2H), 5.04, s, (2H), 5.01, d, (J= 7.6 Hz), (2H), 4.56, d, (J = 12.4 Hz), (4H), 4.24, s, (4H), 4.16, d, (J = 12.4 Hz), (6H), 4.11, d, (J = 15.2 Hz), (4H), 3.87, d, (J = 5.6 Hz), (4H), 3.16, d, (J = 14.8 Hz), (4H), 2.85, s (4H) $^{13}$C-NMR (400 MHz, $C_2D_2Cl_4$, + 140 ˚C) $\delta$ = 157.36, 156.67, 154.00, 136.11, 135.83, 134.92, 134.74, 133.41, 130.00, 129.65, 125.48, 123.06 122.54, 118.74, 116.10, 76.68, 74.84, 73.55, 31.032, 30.782. Anal. Calcd for $C_{62}H_{54}0_6N_2$ : C, 79.8%; H, 5.8%; O, 10.3%; N, 4.1% Found C, 79.6%; H, 5.9%

### 5.8 Alkali Metal Picrate Extractions

All glassware used in the extraction experiments was washed with acetone, Alquinox detergent, and rinsed again with acetone and dried at 110 °C for 24 h prior to dissolution of host. $CHCl_3$ was distilled and washed with deionized water to compensate for the volume changes that occurred. Picric acid was neutralized with the LiOH, NaOH, KOK, RbOH, and CsOH metal hydroxides and recrystallized from ethanol and water (1:1). The crystals were placed in a vacuum desiccator for 48 h and then stored in the dark.[21] Aqueous and organic phases were both examined for consistency. The aqueous solution was diluted so that absorbance values ranging from 0.1 - 1 absorbance units were observed. Absorbance measurements were taken on a Beckman 7000 UV-Vis using an extinction coefficient ($\varepsilon_{354\,mn}$ = 14,500 $cm^{-1}$ $M^{-1}$) in water and ($\varepsilon_{380\,mn}$ = 18,000 $cm^{-1}$ $M^{-1}$) in $CHCl_3$ and $CH_3CN$. In 8 mL glass vials, 2.0 mL of a 1.0 x $10^{-3}$ M (**4, 5,** and **6**) and 5.0 x $10^{-4}$ M (**7**) solution of host dissolved in $CHCl_3$ was delivered (via 2.00 mL glass syringe) along with 2.00 mL (via micropipette) of prepared aqueous metal picrates having concentrations of 9.5 x $10^{-4}$ M, 9.6 x $10^{-4}$ M, 8.4 x $10^{-4}$ M, 1.0 x $10^{-3}$ M, 9.2 x $10^{-4}$ M for $Li^+$, $Na^+$, $K^+$, $Rb^+$, $Cs^+$ ions respectively. The vials were sealed and shaken vigorously for 5 min. and allowed to sit overnight prior to UV analysis at 23°C.

### Determination of Ke and Ka values

The extraction constants (Ke) were calculated from experimental data and the distribution constants (Kd) used have been previously reported.[21] The values of Ka, the host-guest association constant, were calculated from Ke and Kd and the definitions and relationships in the following equations 1-4 wherein H represents the host.

(1) $$[M^+Pic^-]_{org} + [H]_{org} \overset{Ka}{\rightleftharpoons} [M^+*H*Pic^-]_{org}$$

(2) $$[H]_{org} + [M^+]_{aq} + [Pic^-]_{aq} \overset{Ke}{\rightleftharpoons} [M^+*H*X^-]_{org}$$

(3) $$[M^+]_{aq} + [Pic^-]_{aq} \overset{Kd}{\rightleftharpoons} [M^+Pic^-]_{org}$$

(4) $$\mathbf{Ka} = Ke/Kd$$

The physical measurements that were utilized in the calculations of Ka values were as follows:

(5) $$*[Pic^-,H,M^+]_{org} = \{[Pic^-,M^+]_{aq} i - AD/\Sigma\ 1\ \}$$

(6) $$[Pic^-,H,M^+]_{org} = AD/\Sigma\ 1$$

(7) $$[Pic^-,M^+]_{aq} = \{[Pic^-,M^+]_{aq} i - AD/\Sigma\ 1\ \}$$

(8) $$Ke = \frac{[Pic^-,H,M^+]_{org}}{\gamma_{\pm}^2\,([Pic^-,M^+]_{aq})\{([H_{org}i])-([Pic^-,H,M^+]_{org})\}}$$

The formalizations are as follows: Ka and Kd are defined by eq 1 and 3; $Pic^-$ and $M^+$ are the picric and the metal ions of the picric; $[Pic^-,H, M^+]_{org}$ is the host picrate complex concentration in $CHCl_3$ calculated at equilibrium, either from

direct UV measurements, or from the decrease of picrate from water solution. $[Pic\text{-},M+]_{aq}$ represents the alkali cation and picric anion in aqueous phase; $[Pic\text{-},M+]_{aq}$ represents the initial picrate concentration in the aqueous phase; H is the host; A is the observed absorbence; D is the factor at which the aliquots from taken from the $CHCl_3$ or $H_2O$ layers were appropriately diluted; $\gamma^2 = .95$ is the activity coefficient of the picrate in water[21]; $l$ is the light pathlength for the UV cell; $\Sigma$ is the extinction coefficient.

### 5.9 Job Plot Titrations

In the Job plot analysis, 7 solutions of host:guest ratios ranging from 80:20 to 20:80 were prepared in 1 mL volumetric flasks. Aliquots of a 1M NaSCN solution in $CD_3OD$ were added to the flask containing the hosts dissolved in $CDCl_3$. The total solvent composition was then adjusted to be 90% $CDCl_3$ and 10% $CD_3OD$. Spectra of the hosts in the absence of guest were obtained in the 10% $CD_3OD$ solutions so the affect of solvent composition could be quantified.

### 5.10 NMR (other)

In the titration experiments, solutions of the hosts and metal picrate salts were prepared in 1.00 mL volumetric flasks. The solid compounds were placed directly into the flask and $CDCl_3$ was added to the mark. The solutions were stirred for several hours to ensure that all components were dissolved. The solutions were then transferred to NMR tubes and their spectra were recorded at

room temperature. Stack plots of the alkali metals were done by dissolving equal molar amounts of calix[6]arene and alkali metal picrates in a 1.00 ml volumetric flask and allowed to stir overnight. The solution was then filtered through a syringe filter and analysized on NMR.

Free energy of activation values were obtained by variable temperature NMR until coalescence was reached. $C_2Cl_4D_2$ was used as the solvent at higher temperatures and THF-$d_8$ for lower temperatures.

Three dimensional crystals of all four bis-bridged calix[6]arenes were isolated in $CHCl_3$/methanol mixtures.

## 6.0 Conclusion

The bis-bridged calix[6]arenes tested varied in their binding capacities for the alkali metal cations. The four bis-bridged compounds have been analyzed in solid, solution, and gas phases. The two bis-crown-4 conformers exhibited a selectivity trend for the larger cations having the greatest affinity towards $Cs^+$. The two bis-bridged aromatic calix[6]arenes behaved adversely to one another where compound **4** had almost no binding ability while **5** showed very high extraction and binding capabilities for all of the tested alkali metals.

Future work

Transition metals will eventually be tested for their binding performance. Transition metal complexes have could display biomemetric or metaloenzyme like properties. Other bridging units are currently being synthesized, including difunctionalized bipyridinyl, phenanthrolinyl, and salen, all which are capable of selective catalysis. Some initial attempts of a combinatorial approach to optimize synthesis combinations and binding assays have been proposed. Combinatorial analysis will be done primarily using high performance liquid chromatography coupled to an electrospray ionization mass spectrometer.

## References


1 Gutsche, C. D.; Dhawan, B.; No, K. H.; Muthukrishnan, R. *J. Am. Chem. Soc.* **1981**,103, 3782

2 Gutsche, C. D. *Calixarenes* Monographs in Supramolecular Chemistry ed, Vol. 1 ;Stoddart, J. F. The Royal Society of Chemistry: Cambridge, England, **1989**.

3 Gutsche, C. D. *Calixarenes Revisted* Monographs in Supramolecular Chemistry ed;Stoddart, J. F. The Royal Society of Chemistry: Cambridge, England, **1998**.

4 Stewart, D. R.; Gutsche, C. D. *Org. Prep.Proced.Int.* **1993**, 25, 137

5 Cacciapaglia, R.; Casnati, A.; Mandolini, L.; Ungaro, R. *J. Am. Chem. Soc.***1992**,114, 10956

6 Perrin, R. '*New Separation Chemistry Techniques for Radioactive Waste and OtherSpecific Applications*'; Elsevier Applied Science: London; **1991**, p125

7 Diamond, D.; *J. of Inclusion Phenomena and Mol. Rec. in Chem* **1994** 19, 149

8 Ungaro, R.; Pochini, A.; Andreetti, G. D.; Domiano, P. *J. Inclusion Phenom.* **1985**, 3,35.

9 Ugozzoli, F.; Andreetti, G.. D. *J. Inclusion Phenom. Mol. Recognit. Chem.* **1992**, 13, 337

10 van Duynhoven, J. P. M.; Janssen, R. G.; Verboom, W.; Franken, S. M.; Casnati, A.; Pochini, A.; Ungaro, R.; de Mendoza, J.; Nieto, P. M.; Prados, P.; Reinhoudt, D. N. *J. Am. Chen. Soc.* **1994**, 116, 5814

11 Kanamathareddy, S.; Gutsche, C. D.; *J. Org. Chem.* **1994**, 59, 3871

12 Neri, P.; Ferguson, G.; Gallagher, J. F.; Pappalardo, S. *Tetrahedron Lett.***1992**, 33, 7403

13 Kanamathareddy, S.; Gutshe, C. D. *J. Am. Chem. Soc.* **1993**, 115, 6572

14. (a) Kraft, D.; Arnecke, R.; Bohmer, V.; Vogt, W. *Tetrahedron* **1993**, *49*, 6019-6024. (b) Casnati, A.; Jacopozzi, P.; Pochini, A.; Ugozzoli, F.; Cacciapagli, R.; Mandolini, L.; Ungaro, R. *Tetrahedron* **1995**, *51*, 591-598.

15. (a) Arnaud-Neu, F.; Asfari, Z.; Souley, B.; Vicens, J. *New J. Chem* **1996**, *20*, 453-463. (b) Aeungmaitrepirom, W.; Asfari, Z.; Vicens, J. *Tetrahedron Letters* **1997**, *38*, 1907-1910. (c) Pulpoka, B.; Asfari, Z.; Vicens, J. *Tetrahedron Letters* **1996**, *37*, 8747-8750.

16 (a) Araki, K.; Akao, K.; Otsuka,H.; Nakashima, K.; Inokuchi, F.; Shinkai, S. *Chem. lett.* **1994**, 1251. (b) Asfari, Z; Wenger, S.; and Vicens, J. *Supramolecular Science* **1994**, *1*, 103-110. (c) Asfari, Z; Wenger, S.; and Vicens, J. *Pure & Appl. Chem.* **1995**, *67*, 1037-1043. For references on 1,2-alternate calixcrowns see: (d) Arduini, A.; Domiano, L.; Pochini, A.; Secchi, A.; Ungarro, R.; Ugozzoli, F.; Struck, O.; Verboom, W.; Reinhoudt, D. N. *Tetrahedron*, **1997**, 3767-3776. (e) Pappalardo, S.; Petringa, A.; Parisi, M. F.; Ferguson, G. *Tetrahedron Lett.* **1996**, *37*, 3907-3910.

17 Alfieri, C.; Dradi, E.; Pochini, A; Ungaro, R.; Andreeti, G. D. *J Chem Soc., Chem. Commun.* **1983**, 1075 calix crown introduces

18 Nam, K. C.; Park, K. S. *Bull. Korean Chem. Soc.* **1995**, 16, 153-157.

19 (a) Ross, H.; Luning, U. *Tetrahedron Lett.* 1997, *38*, 4539. (b) Ross, H.; Luning, U. *Liebigs. Ann.* 1996, 1367. (c) Ross, H.; Luning, U. *Tetrahedron* **1996**, *52*, 10879.

20 Ugozzoli, F.; Ori, O.; Casnati, A., Pochini, A.; Ungaro, R.; Reinhoudt, D. N. *Supramol. Chem.* **1995**, 5, 179.

21 (a) Ungaro, R.; Arduini, A.; Reverberi, S.; Pochini, A.; Andreetti G.D.; Ugozzoli F. *Tetrahedron* **1986**, vol. 42, No. 7, 2089-2100 (b) Helgeson, R. C.; Weisman, G. R..; Toner, J. L.; Chao, T. Y.; Mayer, J. M.; Cram, D. J.* *J. Am. Chem. Soc.* **1979** 101, 4928 (c) Bourgoin, M.; Wong, K. H.; Hui, J. Y.; Smid, J.* J. Am. Chem. Soc. 1975 97, 3462

22 Moore, S. S.; Tarnowski, T. L.; Newcomb, M.; Cram, D. J.• *J. Am. Chem. Soc.* **1977**, 99, 6398

23 Gutshe, C. D.; Lin, L.-G.; *Tetrahedron* **1986** 42, 6, 1633

24. The x-ray crystal structure for the 1,2,3-alternate conformer **3** was solved, but the R value was only 13%. Even though this is not ideal, it still is sufficient to determine the conformation.

25. (a) Asfari, Z.; Naumann, C.; Vicens, J.: Nierlich, M.; Thuery, P.; Bressor, C.; Lamare, V.; Dozol, J.-F. *New J. Chem.* **1996**, *20*, 1183-1194. (b) Casnati, A.; Pochini, A.; Ungaro, R.; Ugozzoli, F.; Arnaud, F.; Fanni, S.; Schwing,

M.; Egberink, J.; de Jong, F.; Reinhoudt, D. *J. Am. Chem. Soc.* **1995**, *117*, 2767-2777. (c) Ungaro, R.; Casnati, A.; Ugozzoli, F.; Pochini, A.; Dozol, J.; Hill, C.; Rouquette, H. *Angew. Chem. Int. Ed. Engl.* **1994**, *33*, 1506-1508. (d) Ghidini, E.; Ugozzoli, F.; Ungaro, R.; Harkema, S.; El-Fadl, A. A.; Reinhoudt, D. N. *J. Am. Chem. Soc.* **1990**, *112*, 6979-6985.

26 Feeney, J.; Batchelor, J.G.; Albrand, J. P.; Roberts, G. K. *J. Magn. Reson.* **1979**, *33*, 519.

27 Matsumoto, H.; Shinkai, S. *Tetrahedron Letters* **1996**, *37*, 77-80.

28. Blanda, M. T.; Farmer, D. B.; Brodbelt J. S.; Goolsby, B. unpublished results

29 (a) Blair, S. M., Kempen, E.C., Brodbelt, J.S., *J. Am. Soc. Mass Spectrom.*, **1998**, 9, 1049-1059.; (b) Blair. S.M., Brodbelt, J.S., Reddy, G.M., Marchand, A.P., *J. Mass Spectrom.*, **1998**, 33, 721-728; (c) Kempen, E.C., Brodbelt, J.S., Bartsch, R.A., Jang, Y., Kim, J.S., submitted to *Anal. Chem.*, **1998**; (d) Gooslby, B.J., Brodbelt, J.S., Adou, E., Blanda, M.T., submitted to Int. *J. Mass. Spectrom.*, **1999**.

30 Geraci, C.; Chessari, G.; Piattelli, M.; Neri, P* *Chem. Commun.* **1997** p 9-10

31 Casnati, A.; Pochini, A.; Ungaro, R.; Ugozzoli, F.; Arnaud, F.; Fanni, S.; Schwing, M.-J.; Egberink, R. J. M.; de Jong, F.; Reinhoudt, D. N. *J. Am. Chem. Soc.* **1995** 117, 2767

32 Atta-ur-Rahman *Nuclear Magnetic Resonance* Springer-Verleg: New York **1986**, pp 131-133

**Appendix**: Spectra

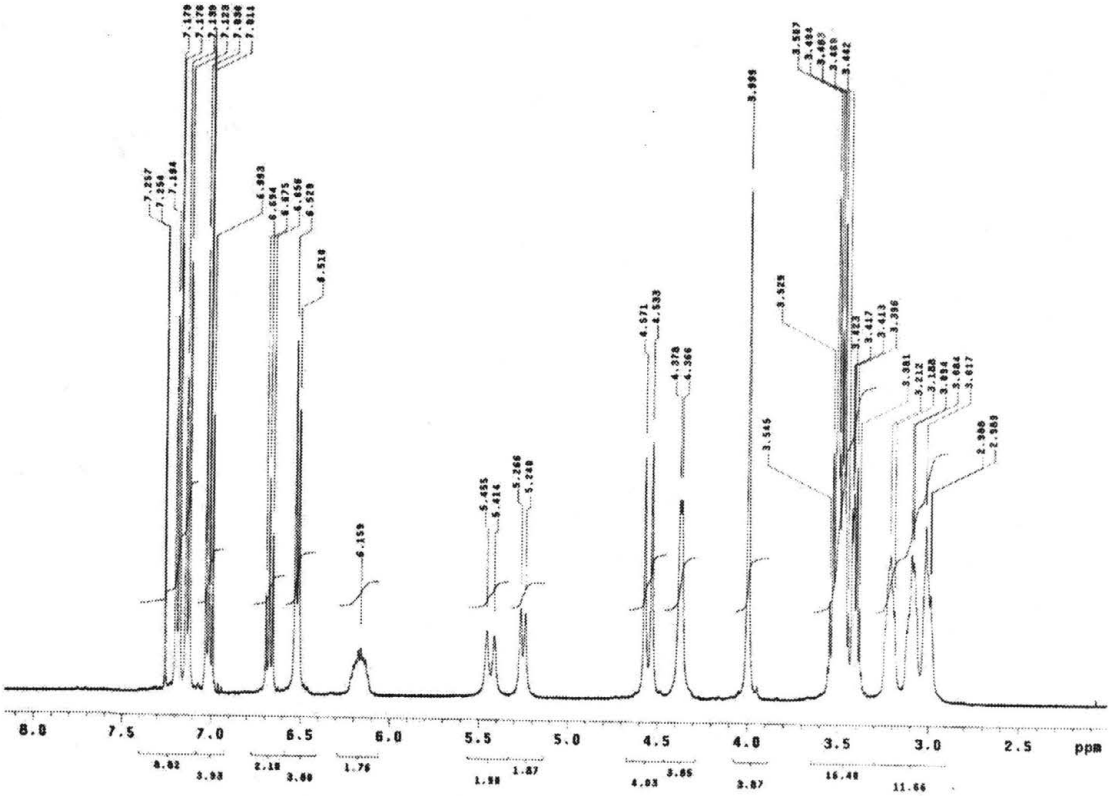


**Spectra 1** *[1]H-NMR of compound* ***4***

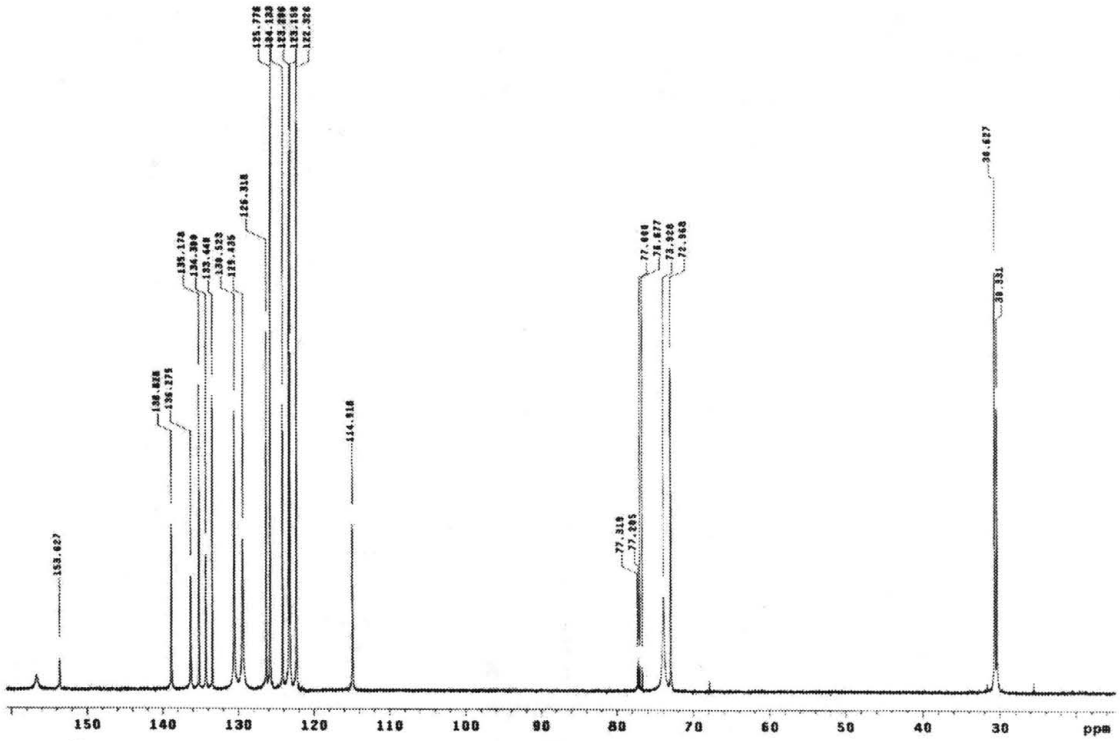


**Spectra 2** *[13]C-NMR of compound* ***4***

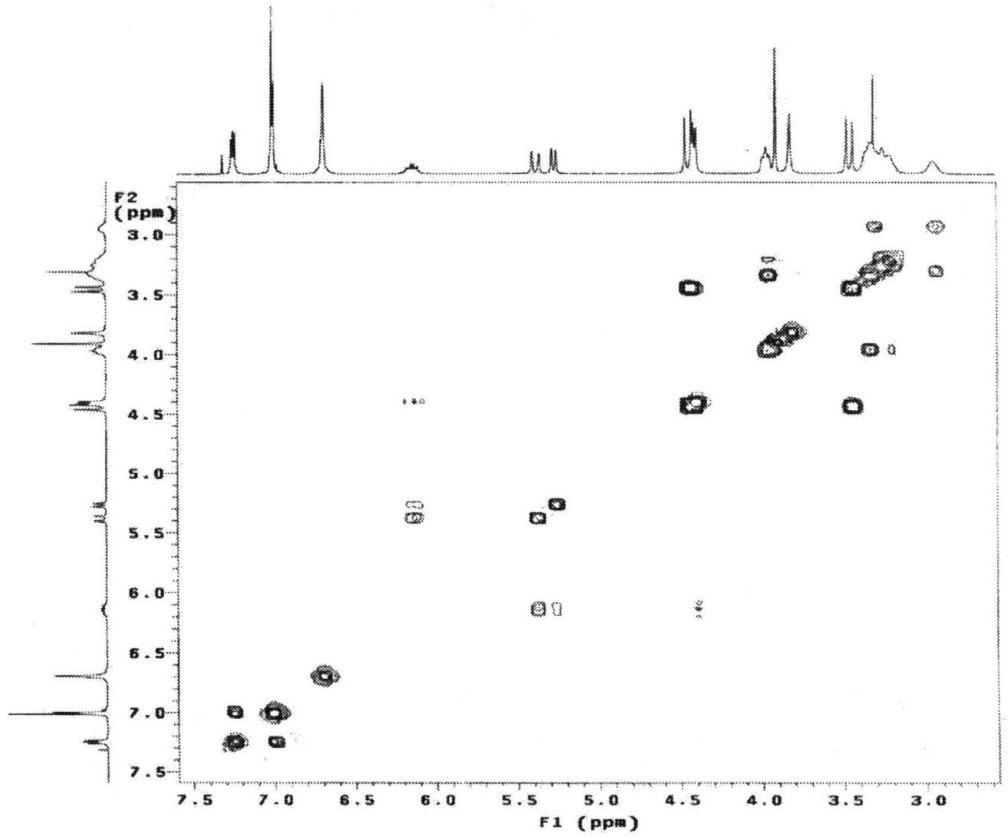


**Spectra 3** *Cosy-NMR of compound* ***4***

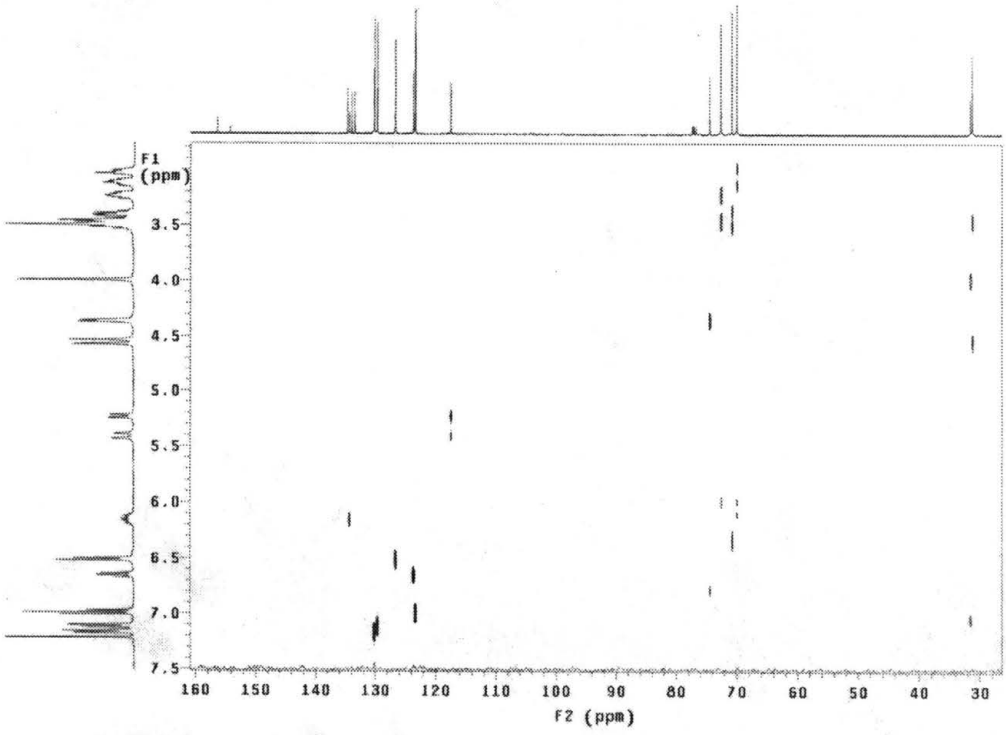


**Spectra 4** *Hetcor-NMR of compound* ***4***

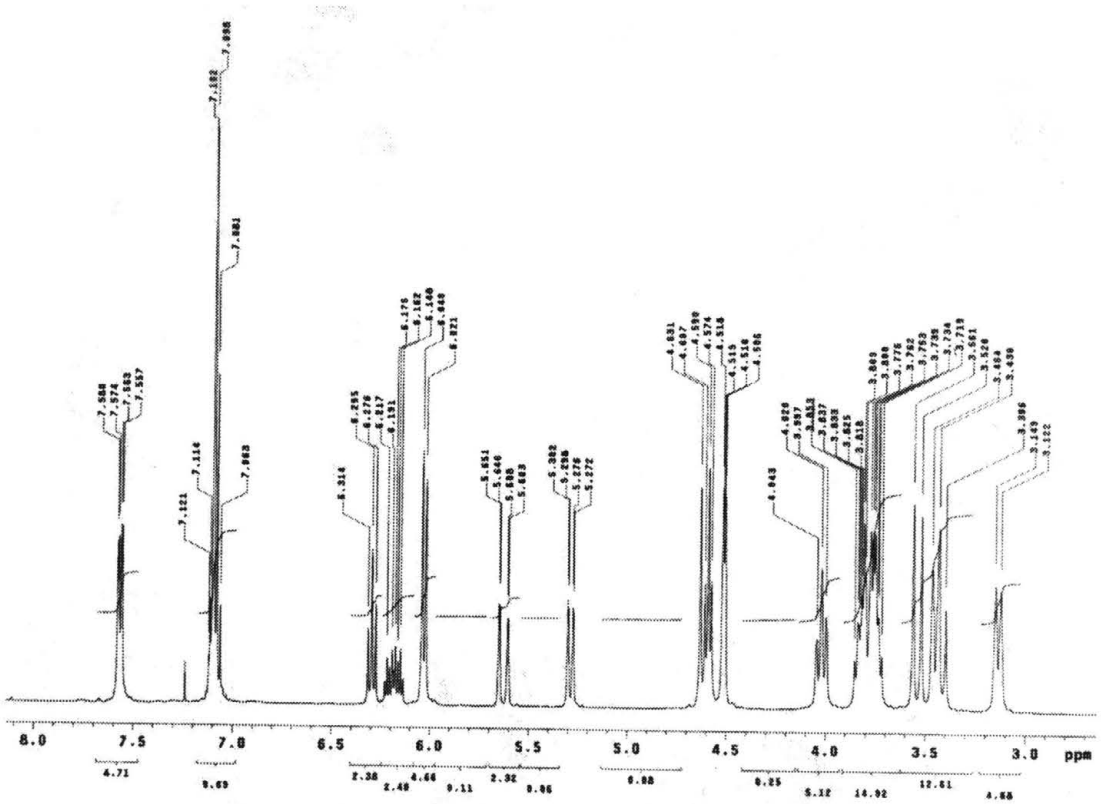


**Spectrum 5** *[1]H-NMR of compound 5*

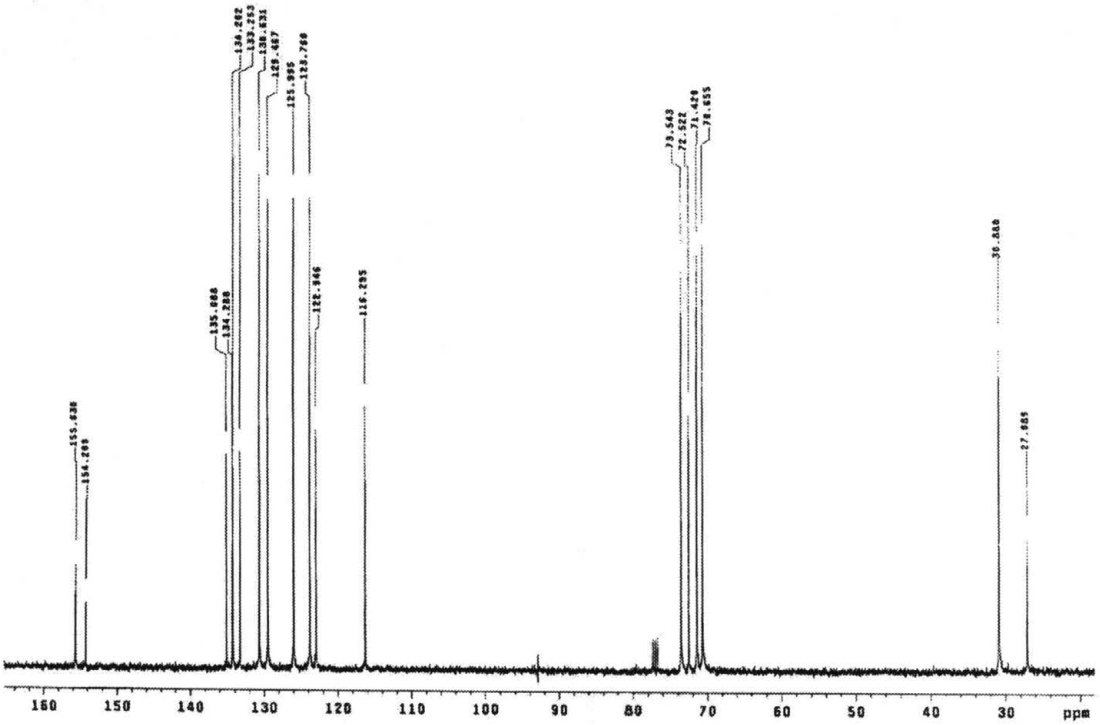


**Spectrum 6** *[13]C-NMR of compound 5*

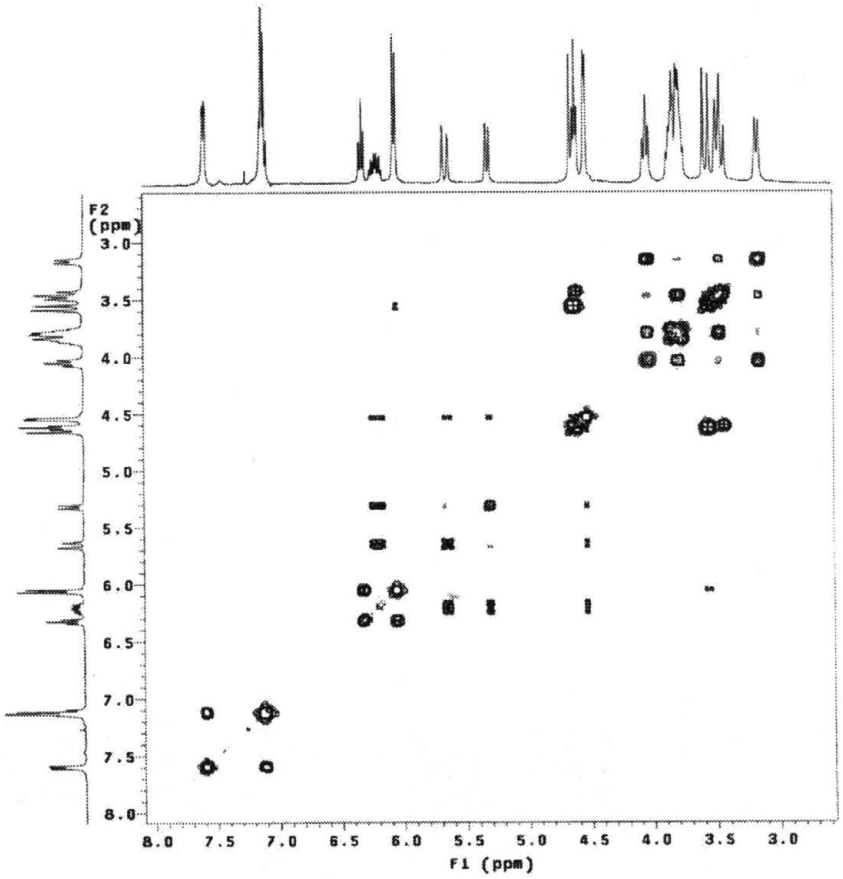


**Spectrum 7** *Cosy-NMR of compound* ***5***

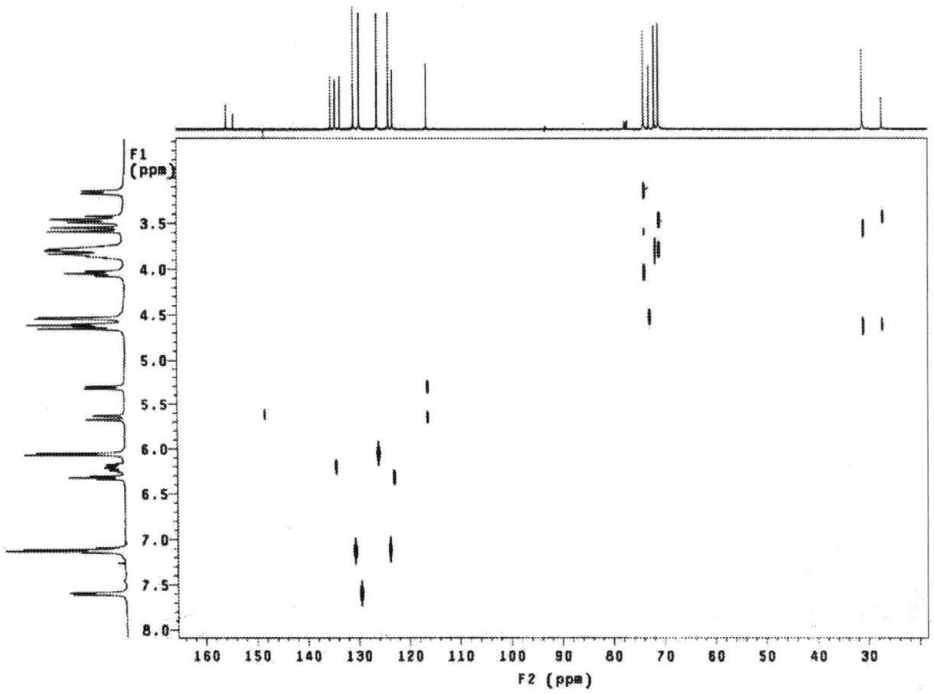


**Spectrum 8** *Hetcor-NMR of compound* ***5***

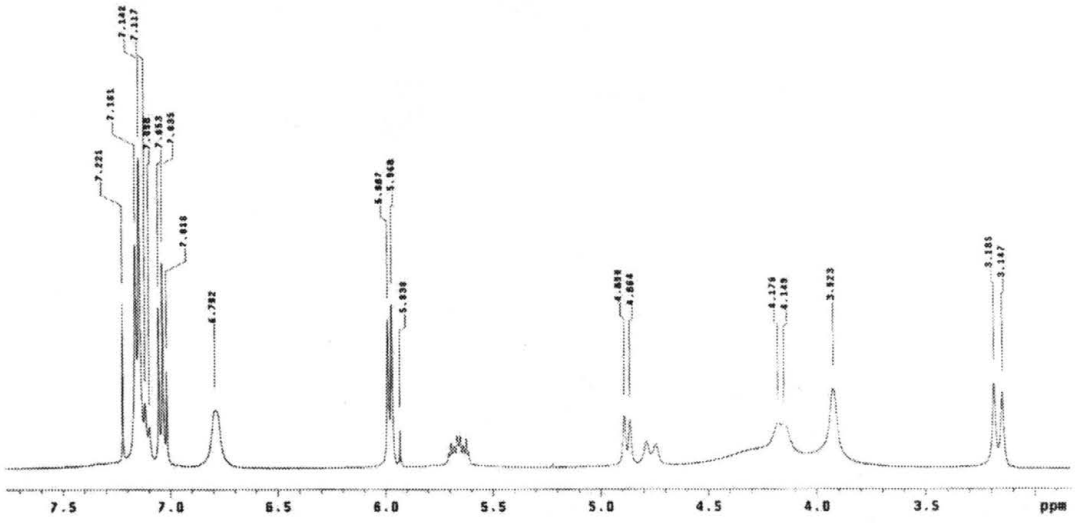


**Spectum 9** *$^{1}$H-NMR of compound **6**.*

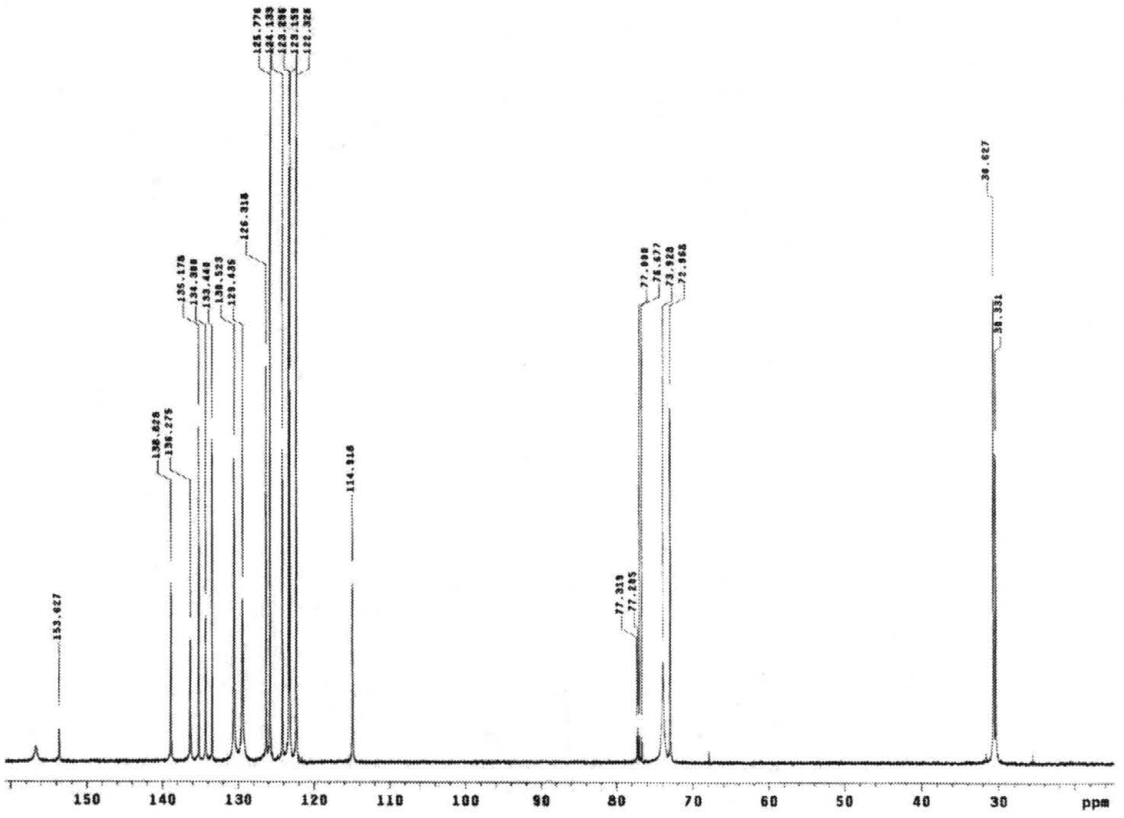


**Spectrum 10** *$^{13}$C-NMR or compound **6**.*

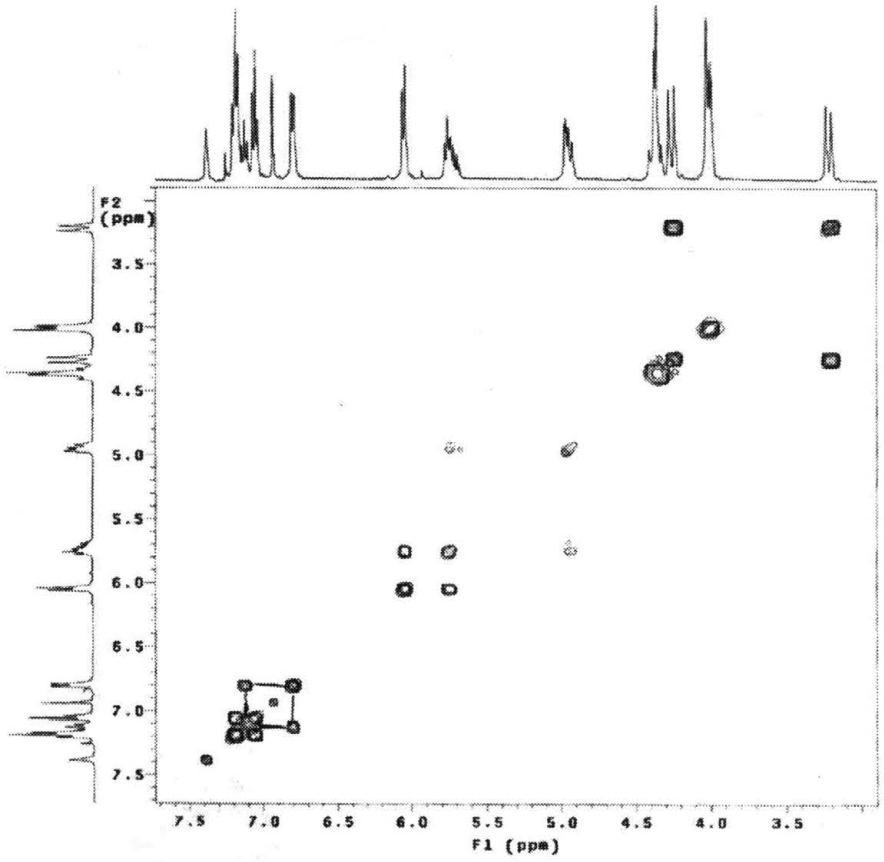


**Spectrum 11** *Cosy-NMR compound **6**.*

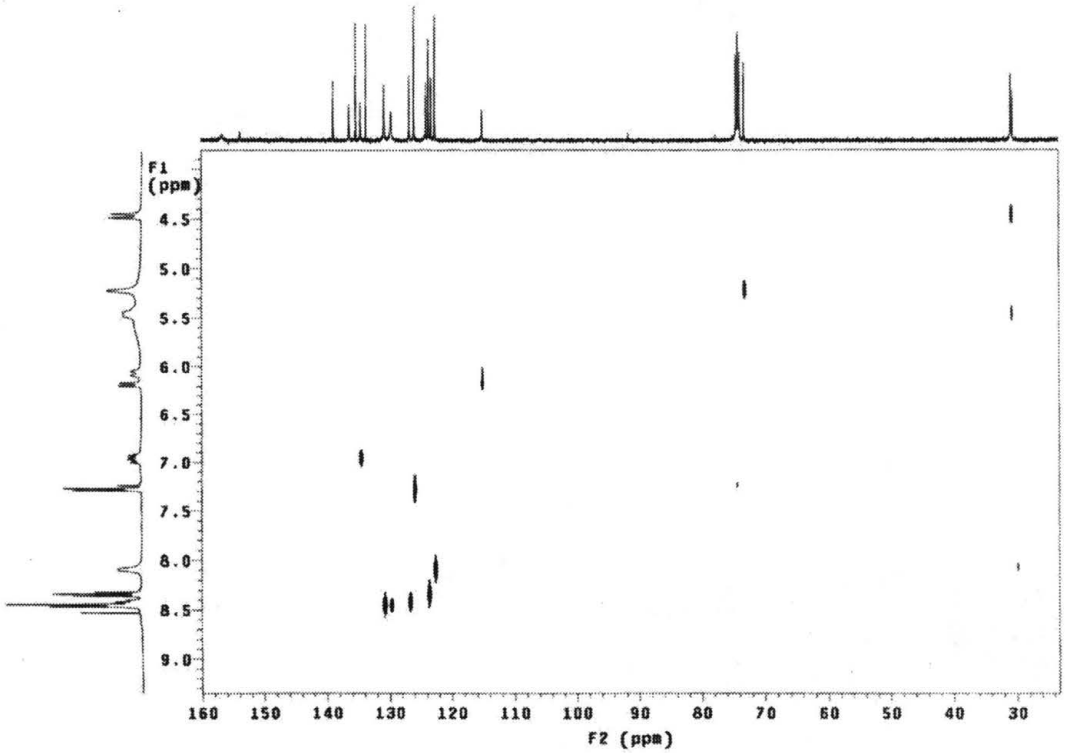


**Spectra 12** *Hetcor-NMR of compound **6***

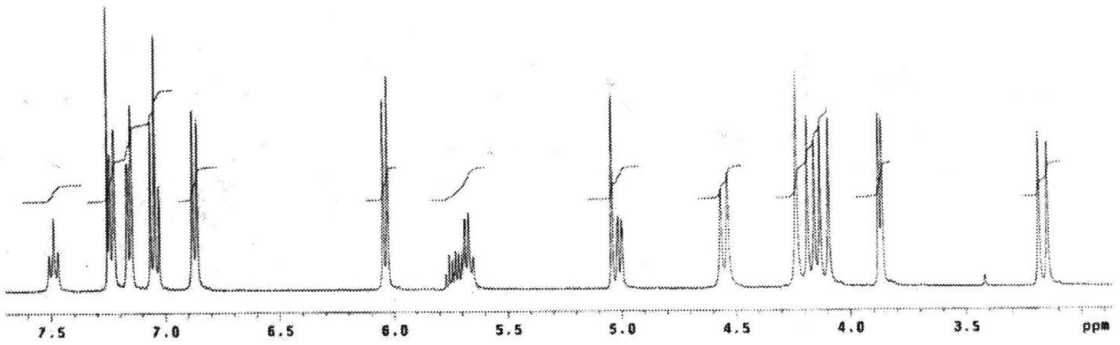


**Spectra 13** *$^{1}$H-NMR of compound 7*

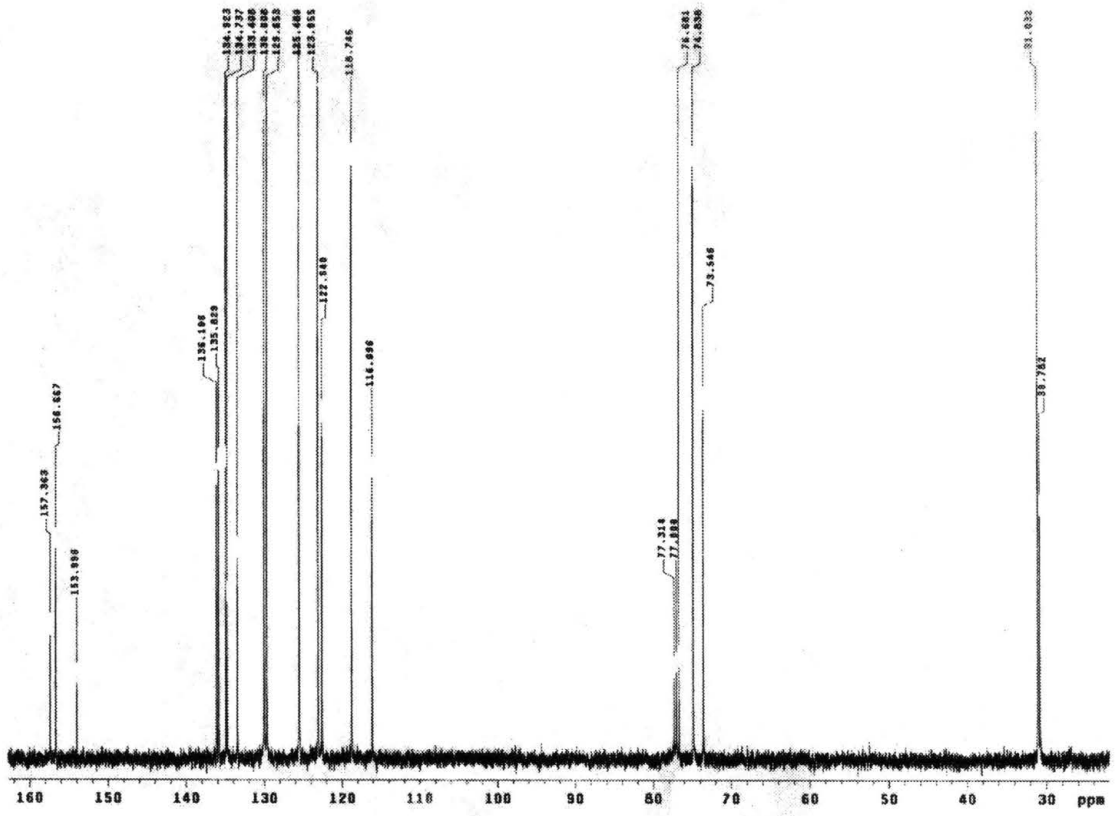


**Spectra 14** *$^{13}$C-NMR of compound 7*

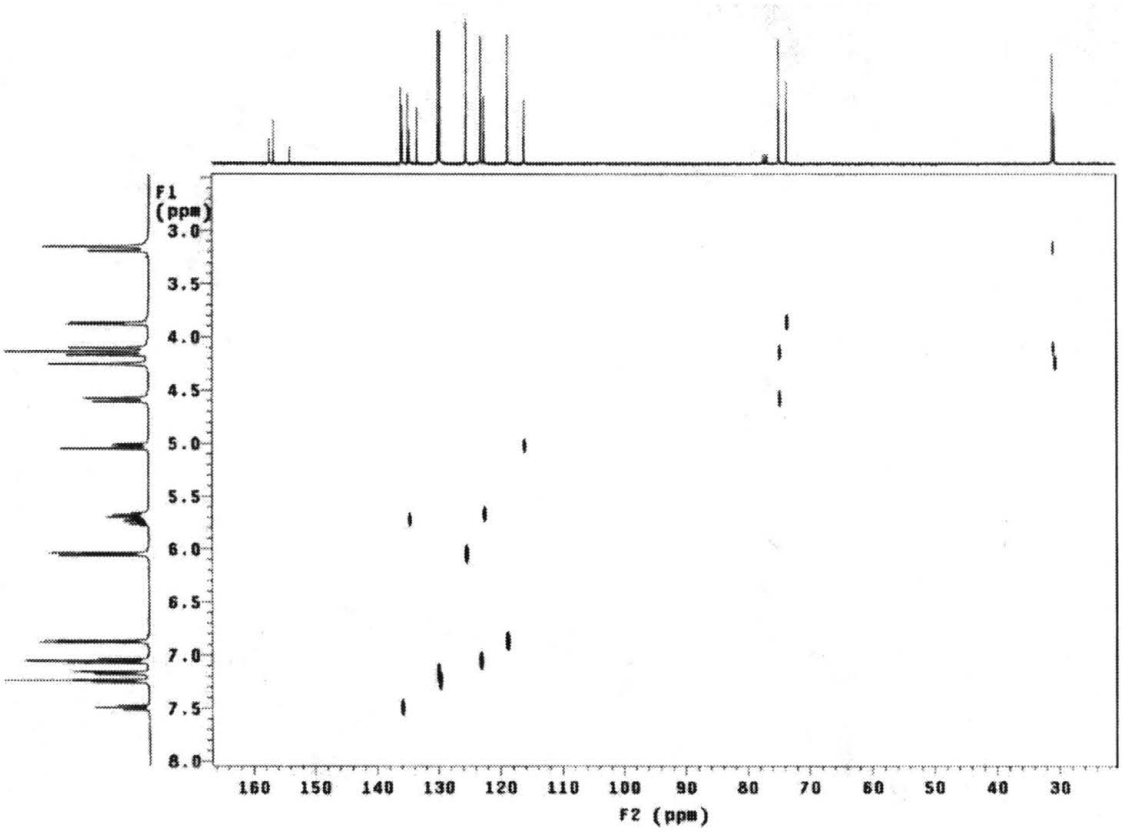


**Spectra 15** *Hetcor of compound 7*

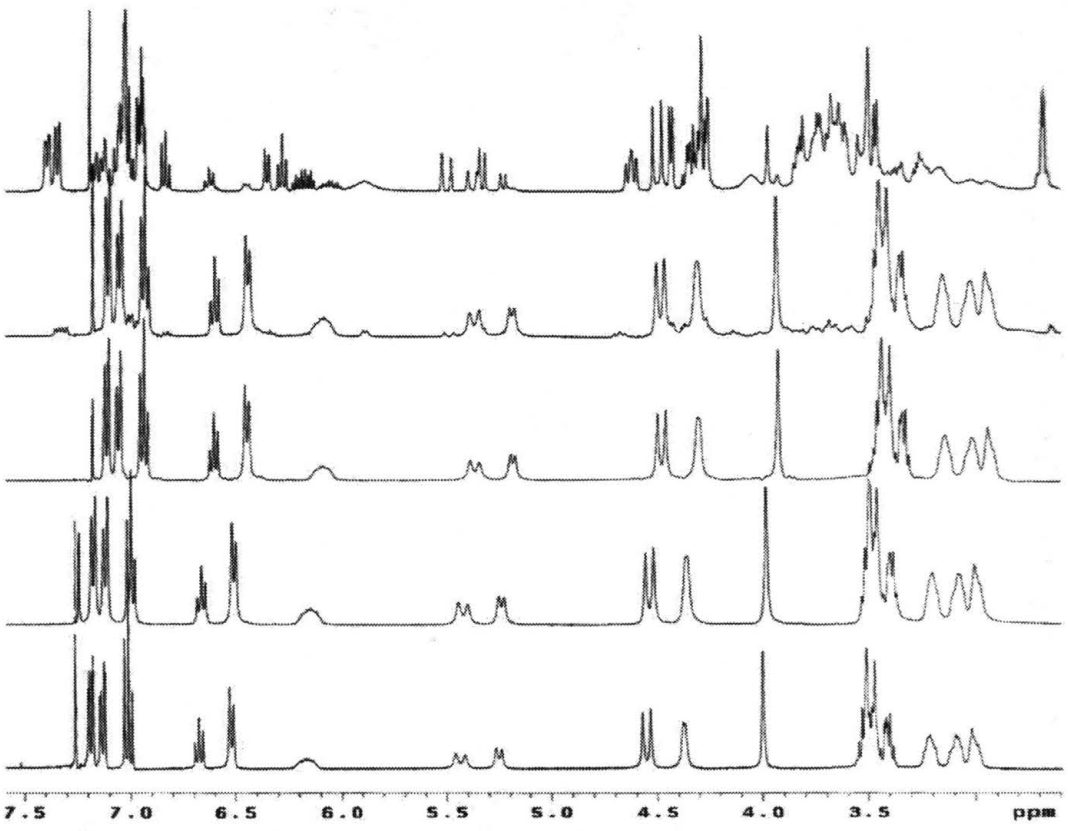


**Spectrum 16** *Stack plot of $Cs^+$, $Rb^+$, $K^+$, $Na^+$. and Free Host* ***4***

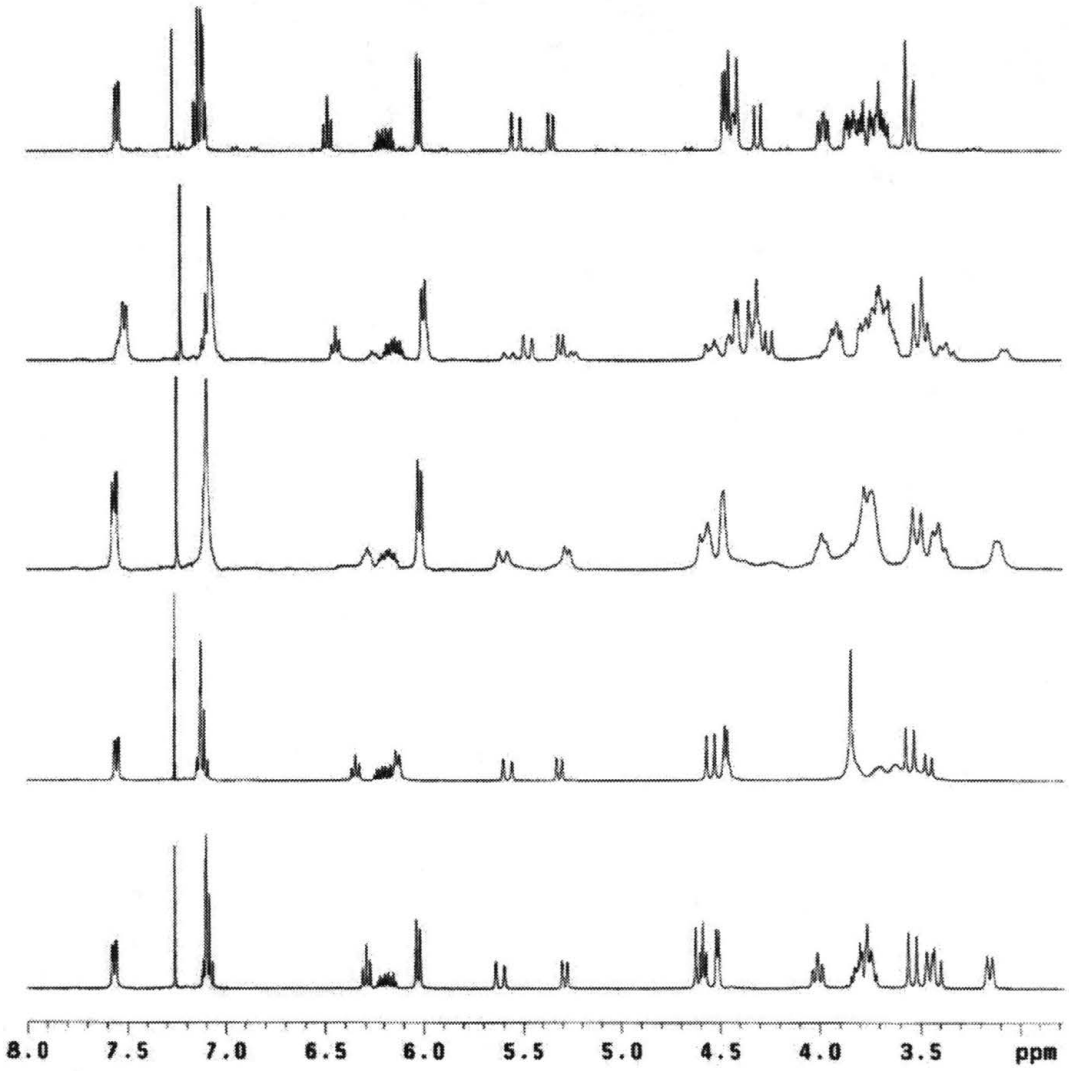


**Spectum 17** *Stack plot of $Cs^+$, $Rb^+$, $K^+$, $Na^+$. and Free Host* ***5***